Materials and Methods

Drug screening platform: The combination drug screen was performed by plating 5,000 cells per well in each well of twenty-six 96-well black clear bottom plates in 180 μL of media. After 24 hours of incubation, drugs were diluted from a master stock and each plate of cells was drugged bringing the total volume of each well to 200 μL. Each drug was tested at 9 concentrations, and at a concentration of 0, in the presence or absence of the appropriate concentration of each primary TKI: gefitinib (1 μM), crizotinib (1 μM), lapatinib (1 μM), PHA665752 (1 μM), dacomitinib (1 μM), WZ4002 (1 μM), ceritinib (0.3 μM) as indicated in Tables S3 and Table 2. Patient-derived lines with secondary mutations in the primary oncogene (EGFR T790M or ALK L1196M) were screened with a compound that inhibits the target despite the mutation (WZ4002 or ceritinib, respectively). Each step of the titration diluted the previous concentration by the square root of 10 for a total concentration range of 10,000-fold tested. After incubation for 72 hours in drug, cell counts were determined using CellTiter-Glo (Promega) as per manufacturer's instructions.

Analysis of screen data: Each plate was normalized to the mean of the six conditions on the plate with a screen drug concentration of 0 (values for the plates with TKI are normalized to the 6 TKI only wells). After normalization, best-fit lines and the resulting GI50s were calculated using GraphPad Prism [log(inhibitor) vs normalized response]. The maximum GI50 determined was capped at the maximum dose of drug administered to eliminate extrapolated values. The AUC of each curve was determined using GraphPad Prism ignoring regions defined by fewer than 2 peaks. Fold-change (GI50) was determined as follows: (GI50 single agent drug)/(GI50 combination drug). Percent change AUC was calculated as follows: [(AUC single agent drug-AUC combination drug)/(AUC single agent drug)]*100. To determine the threshold to call a hit we performed long-term viability assays on a subset of 10 cell lines with 11 different drugs (Fig. S16A) and determined the extent to which each drug combination tested impeded cell viability. We selected thresholds allowed the identification of effective combinations with an acceptably low likelihood of pursuing false positives (Fig. S16B). Hits were called when the change of AUC exceeded 10% and the fold-change GI50 exceeded 4; these thresholds correspond to a specificity of 0.93 and a sensitivity of 0.46. See Fig. S16B for ROC curves. Synergism was evaluated using the Bliss independence model with the expected effect of drug combination corresponding the product of the viability ratios observed for each single agent and excess over bliss corresponding to the difference between the expected viability and the observed combination effect. Excess = (Vs_obs_1x Vs_obs_2) – Vc_obs1,2. With Vs_obs_1 the viability ratio (Treated / DMSO control) observed with drug 1, Vs_obs_2 the viability observed with drug 2 and Vc_obs1,2 the viability observed for the combination using the same drug concentrations than for the single agents. The average excess over bliss across the 9 concentrations tested is reported as a percentile of viability. Bliss synergism calculations were performed using data collected independently of the primary screen. Triplicate measurements were used for these experiments.

Primary TKI sensitivity assays: Dose-response assays to determine the effect of a given screen drug on the sensitivity to the primary TKI are done identically to the primary screen platform however each data point was performed in triplicate and each experiment was repeated three times. Unless otherwise stated, a representative result is presented. Best fit curve is generated in GraphPad Prism [(log (inhibitor) vs response (three parameters)]. Error bars are mean -/+ SEM.

Western blotting: Lysates were prepared as previously described (*28*). Antibodies against pALK, tALK, pMEK, pERK, tERK, pAKT, tAKT, p-PRAS40, pS6, tS6, BIM, pPaxillin and Actin were purchased from Cell Signaling Technology. Antibody against pEGFR was purchased from AbCam. Antibody GAPDH was purchased from MilliPore.

Fluorescence in-situ hybridization: Performed as previously described **(*18*).**

Quantitative PCR: MET gene copy number was measured via a quantitative PCR assay with each reaction containing 10 ng of gDNA with SYBR green master mix (Roche) and a primer pair designed to amplify MET exon 17. Reactions were run on a LightCycler 480 (Roche) for quantitation. LINE-1 was used as a loading control and normal female gDNA was used as a diploid control.

Long-term viability assays: 1,000 cells per well were plated on 96-well black clear bottom plates in a total volume of 180 μL/well. 5 replicates were done of each condition. At 24 hours, one plate of cells was frozen (-80ºC) representing the time 0 plate. At this time the remaining plates were brought to the indicated drug concentration by adding 20 μL of media at 10X the final concentration. After incubation for 72 hours, the media was replaced and new drug was added. After 144 hours each of the plates was frozen (-80ºC). After freezing, the plates (day 6 and time 0) were thawed simultaneously, and cells were quantified using CellTiter-Glo (Promega). The reported "Cell change %" was determined as follows: 100*(Value/Baseline)/Baseline. Each point performed with 5 replicate. Unless otherwise noted, 3 independent experiments were performed and a representative result in presented. Error bars are mean -/+ SEM.

Crystal Violet: Cells were plated at a density of 100 – 200k/well of a 6-well plate. Cells were drugged the following day and then again 72-96 hours after. After 1 week in drug, cells were fixed with gluteraldehyde for 10 minutes. Post fixation, cells were gently washed 2x with H_20. For staining, add 2 mls of 0.1% crystal violet and incubated for 30 minutes. Cells were then washed 3x with H_20. Plates were inverted and dried overnight. Images were taken the next day and plates were quantified by using 10% acetic acid to extract the stain and absorbance read at 590nm.

Apoptosis Assays: Cells were plated on 96-well plates. Each condition was performed in triplicate. Drug was added to cells 24 hours after seeding for 48 hours. Caspase cleavage was quantified using ApoTox-Glo Triplex Assay (Promega). Relative caspase cleavage was determined as follows: (luminescence)/[400Ex/505Em (Viability)]. For flow cytometric apoptosis assays cells were treated for 72 hours then analyzed. Cells were washed in PBS then trypsinized. All material was collected, combined, centrifuged at 15,000 rpm for 5 min and washed with PBS. Pellets were resuspended with 500 μL annexin V binding buffer and stained with annexin V and propridium iodide (PI). Analysis was performed on a BD Biosciences LSRII flow cytometer. All presented apoptosis assay were performed in triplicate, and three replicate experiments were performed. A representative result is presented. Error bars indicate SEM.

Protein expression and knockdown: wt-SRC (gift of Pieter Eichhorn) and c-SRC K295R (Addgene plasmid 17678, gift of David Shalloway) were cloned into pENTR/D-TOPO Cloning Kit (Invitrogen), which was used to raise lentivirus per Broad Institute Protocol. Cells were infected following Broad Institute Protocol and selected with puromycin for at least 72 hours before all experiments. For SRC knockdown experiments hairpins NM_198291.1-3496s1c1 (#6) and NM_198291.1-1711s1c1 (#8) were utilized.

Xenografts: All mouse xenograft experiments were performed in male Nu/Nu mice of matching age, 8-12 weeks. A suspension of 5-10 x 10_6 cells resuspended in PBS mixed 1:1 with BD Matrigel Basement Membrane Matrix was inoculated in the subcutaneous right flank. Mice were maintained in laminar flow units in aseptic condition and the care and treatment of all mice was in accordance with institutional guidelines. Tumor size was measured by caliper twice weekly and weights were determined weekly. Volume was calculated as follows: (length*(width^2)*(0.51). Treatment was initiated when a tumor exceeded 150 mm^3. Each drug was prepared in the following solvent: **Gefitinib** [polysorbate (1% Tween 80 in PBS)], **AZD0530 (**0.5% HPMC and 0.1% Tween 80), **Crizotinib** (0.1N HCl), **ceritinib (**0.5% Methyl Cellulose and 0.5% Tween 80), **AZD6244** [0.4% Polysorbate (1% Tween 80 in PBS] and 0.5% of Methyl Cellulose (0.5% HPMC and 0.2% Tween 80). **Dacomitinib** (lactate buffer), **ABT263 (**60% of Phosal 50 PG, 30% of PEG 400*, 10% of 100% EtOH). Drug was administered by oral gavage using a rubber tipped gavage needle. When combinations were administered one hour elapsed between drug doses.

Tumor line derivation: Patient-derived models were developed with the fibroblast feeder system (*11*) or were cultured with collagen-coated plates in ACL4, RPMI, or DMEM medium. The feeder cells were irradiated fibroblasts (5000 rad) from normal patient tissue. Models derived using the feeder system were passaged in these conditions until a tumor majority was observed, at which time they were passaged off of the feeder into ALC4, RPMI, or DMEM medium. Development was considered complete when models were independent of the feeder system, free of stromal cells, and determined to maintain known patient tumor mutations.

***In vitro* drug-resistant cell lines derivation:** To derive models of acquired resistance we followed previously described protocols (*29*). In short, parental cell lines were passaged in slowly increasing concentrations of the appropriate drug beginning at approximately IC10. Media was refreshed twice weekly and cells split at subconfluence. When cells grew freely in the given concentration of drug the concentration was increased in a stepwise manner, and the process was repeated until a concentration of drug known to completely or nearly completely inhibit the intended target was achieved.

Gene expression analysis: Cell lines were treated for 24 hours with the indicated drug or vehicle, then RNA was prepared. mRNA expression of patient-derived cell lines was measured with Affymetrix HGU 133 plus 2 microarrays. RMA normalization was performed with the function *justRMA* from the R package *affy* (*30*). We assessed differential expression between cell lines treated with an ALK inhibitor (crizotinib or ceritinib) and vehicle-treated cell lines using *limma (31)*, correcting for the cell line using the following the linear model: expression ~ cell line + treatment. We selected probe sets with a Benjamini-Hochberg corrected p value for the treatment variable of less than 0.1; furthermore, cutoffs on log 2 fold-change of 0.5 and -0.5 were used to define a list of upregulated and downregulated probe sets with treatment, respectively (Database S6)**.** We submitted the upregulated and downregulated gene lists to Gene Ontology analysis using DAVID (*32*) (Database S7 and S8). The gene ontologies the most enriched within genes upregulated upon ALK

inhibition were extracellular matrix and basal membrane (Benjamini p values 1.75E-04 and 2.31E-04). The ontology the most enriched in downregulated genes corresponded to the cell cycle.

Next-Generation Sequencing: NGS library construction was performed with Illumina-compatible sequencing adaptors (Elim BioPharm, Hayward, CA). RNA bait-based hybridization capture was performed with a set of oligonucleotides to capture over 1000 known cancer genes (RightOn Cancer Sequencing Kit, developed in collaboration with Elim BioPharma). Sequences were aligned with BWA-MEM, run through Firehose (Broad Institute) pipeline. Single nucleotide variations are presented when either of the following criteria are met: (1) the mutation is present in less than 6 reads in the control sample and greater than 10 reads in the tested sample, the mutation is in a coding domain, the mutation results in either a missense or nonsense mutation and the mutation is not a known SNP according to the 1,000 Genomes Project or is present is less than 1% of tested alleles and the mutation has been reported in COSMICv68 or (2) the mutation is present in less than 6 reads in the control sample and greater than 10 reads in the tested sample, and the mutation is a nonsense mutation in a tumor suppressor gene (*33*). Mutations reported in MLL3 and NOTCH2 were not reported due to known due to known technical error sequencing these genes.

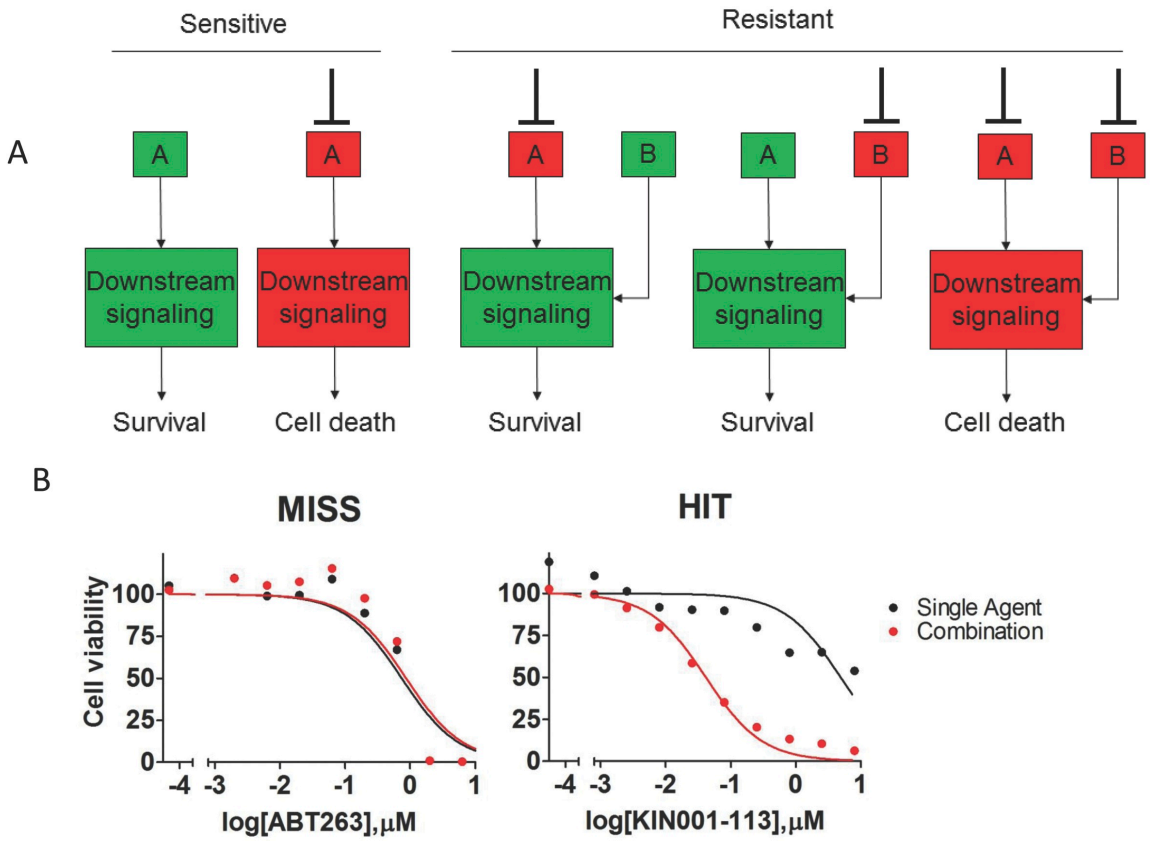

Fig. S1: **Representation of drug screen rationale. A.** Schematic representing the concept of a bypass track in the setting of acquired resistance. In a sensitive cancer, inhibition of the primary oncogene ('A') is sufficient to suppress downstream signaling and cause cell death. In cancers with acquired resistance through bypass track acquisition both the primary oncogene ('A') and the secondary pathway ('B') must be inhibited simultaneously. **B.** Presentation of primary screen data in H2228 PFR1 cells demonstrating a screen miss and a screen hit. The primary screen data for BCL-2 family inhibitor ABT263 is presented as an example of a screen "miss" and the multi-targeted kinase inhibitor KIN001-113 is presented as an example of a screen "hit". The best-fit line represents the variable slope [log(inhibitor) vs. response].

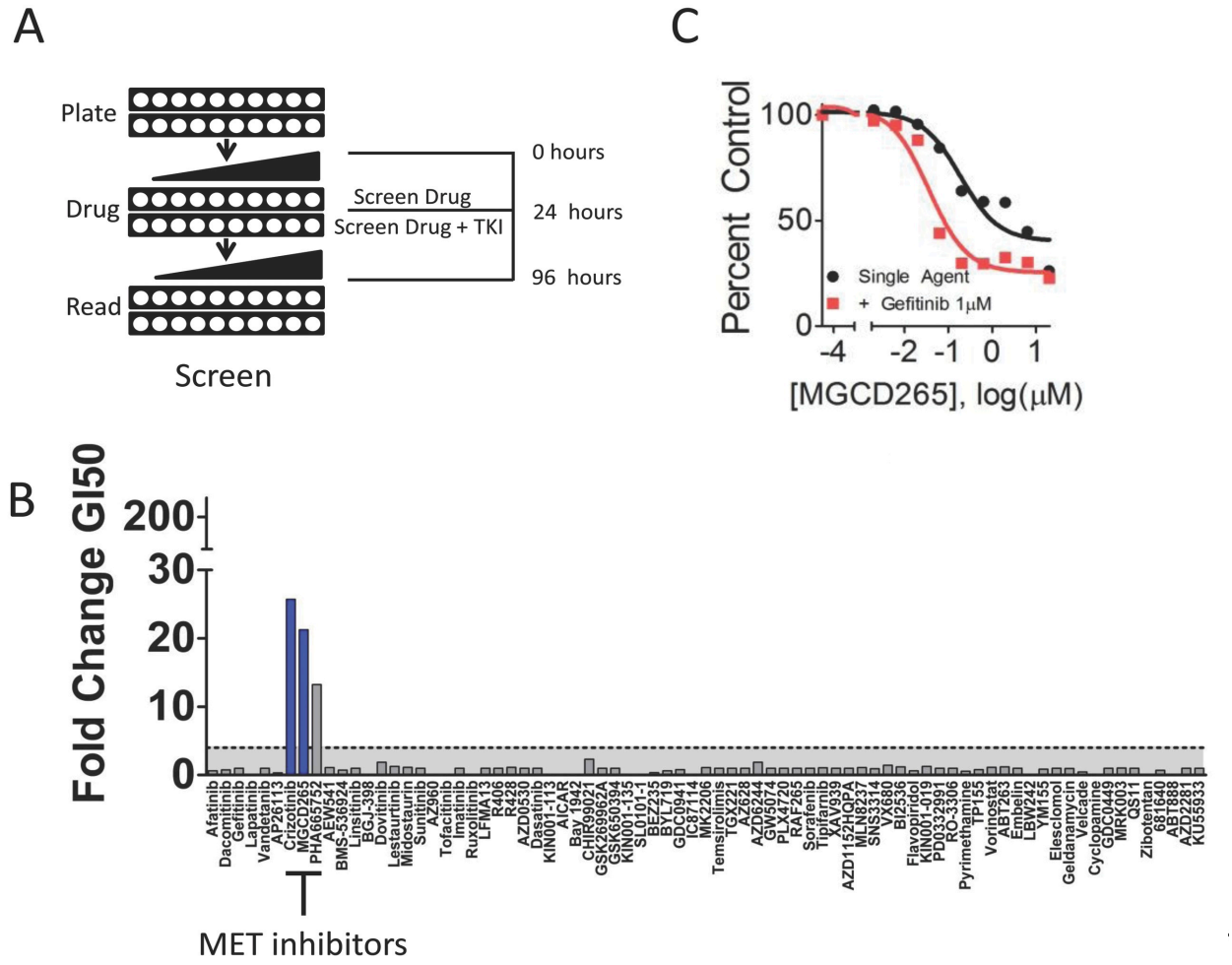

Fig S2: Screen schematic and proof of concept. A. Schematic of the screen workflow. Screen drugs were tested as single agent and in the presence of a single fixed concentration of the primary TKI across 10 concentrations encompassing a 10,000-fold dilution range. After 72 hours, cell viability was determined with CellTiter-Glo. **B.** Representation of screen data for all compounds tested against HCC827 GR6. The y-axis represents the fold-change GI50 that resulted with addition of gefitinib (GI50 single agent/GI50 combination). The bars are color-coded blue when the percent decrease in AUC from single agent to combination was greater than 10%. **C.** An example of primary screen data for the HCC827 GR6 cell line (EGFR-mutant cell line with MET bypass track previously described (*13*)). The MET inhibitor MGCD265 was more potent in combination with 1 μM gefitinib (in red) than as single agent (in black).

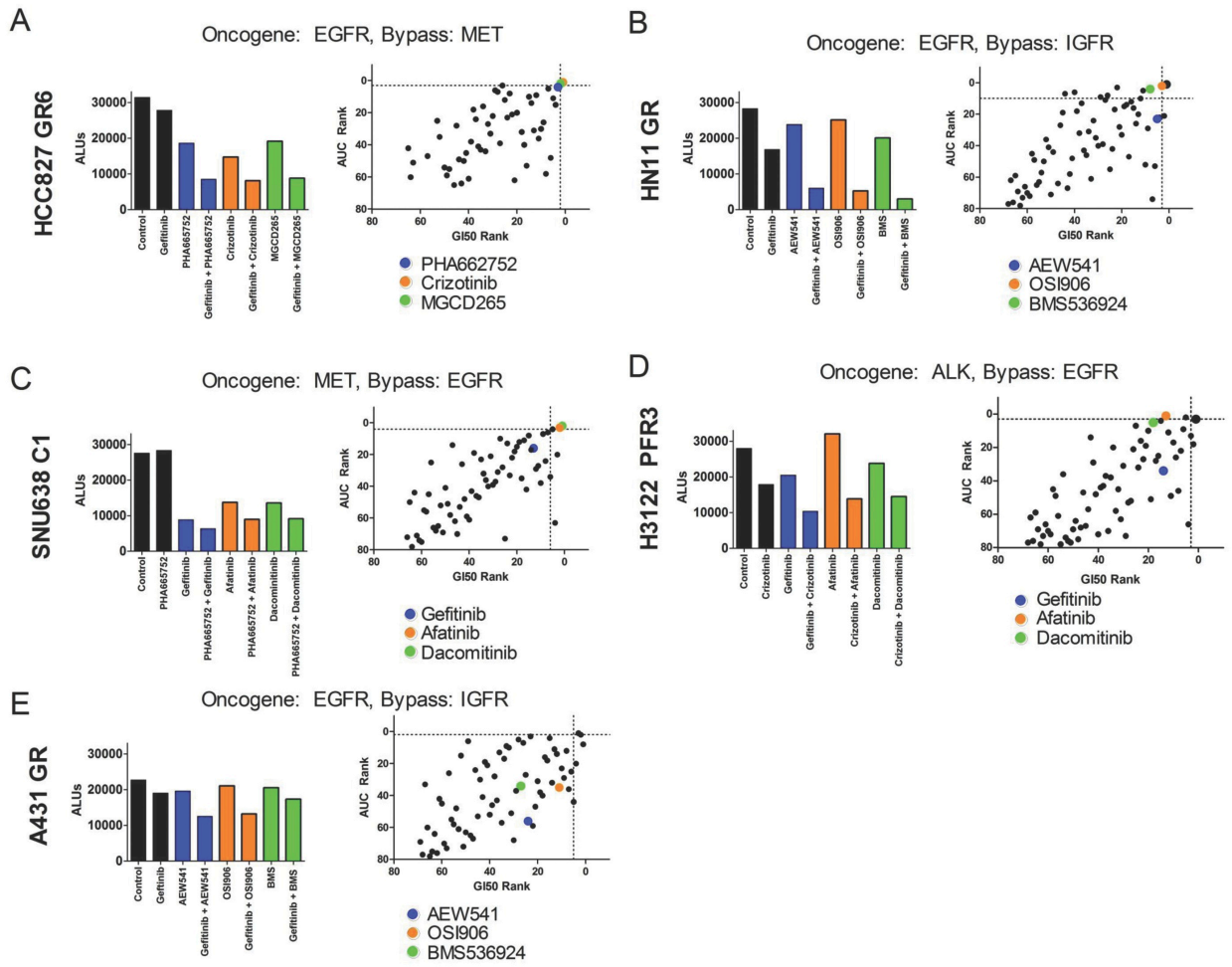

Fig. S3: **Demonstration of the effect of relevant drugs in models with known bypass tracks.** Primary screen data representing all screen drugs across each presented cell line. On the left, each drug was ranked in ascending order from greatest to least fold-change in GI50 and similarly for change in AUC. Each dot represents a single drug. The dotted lines represent where the hit criteria fell: Fold-change GI50 > 4, AUC change > 10%. On the right, the effect of the indicated drug on cell viability [arbitrary luminescence units (ALUs)] is presented. Presented for each line are the screen drugs that target previously published bypass tracks. Also presented are the effects of each drug-model combination on cell viability. Five resistance models are shown: **A.** HCC827 GR6 (EGFR model with MET bypass track): Blue - PHA665752, Orange – Crizotinib, Green – MGCD265. **B.** HN11 GR (EGFR model with IGFR bypass track): Blue – AEW541, Red – OSI906, Green - BMS536924. **C.** SNU638 C1 (MET model with EGFR bypass track): Blue – Gefitinib, Red – Afatinib, Green – Dacomitinib. **D.** H3122 PFR3 (ALK model with EGFR bypass track): Blue – Gefitinib, Red – Afatinib, Green – Dacomitinib. **E.** A431 GR (EGFR model with IGFR bypass track): Blue – AEW541, Red – OSI906, Green - BMS536924.

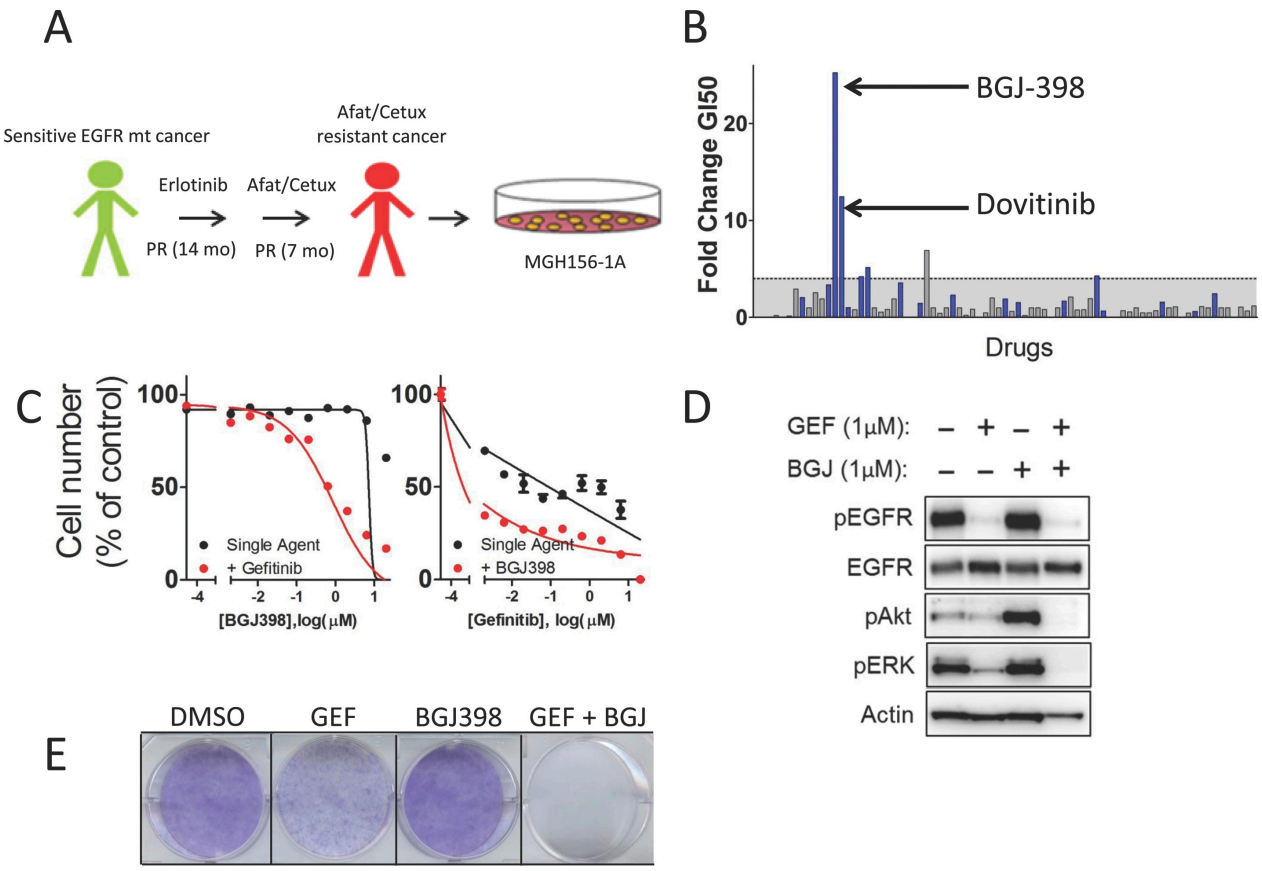

Fig. S4: FGFR3 mutation is a resistance mechanism in a patient derived model: A. Schematic demonstrating the derivation of MGH156-1A from a patient resistance to EGFR inhibitors. B. Representation of screen data for all compounds tested against MGH156-1A. The y-axis represents the fold-change GI50 that resulted with addition of gefitinib (GI50 single agent/GI50 combination). The bars are color-coded blue when the percent decrease in AUC from single agent to combination was greater than 10%. **C**. Left: The FGFR inhibitor BGJ-398 was more potent in combination with 1 μM gefitinib (in red) than as single agent (in black). Synergy was observed with on average 12% less viability than expected across 9 concentrations and a maximum over Bliss of 24% viability effect. Right: BGJ-398 (1 μM) re-sensitizes the MGH170-1BB cells to gefitinib. Error bars are mean -/+ SEM. **D.** Western blot analysis of MGH156-1A. Cells were treated with vehicle, gefitinib (1.0 μM), BGJ-398 (1 μM) or the combination of both drugs for 6 hours. Lysates were analyzed with antibodies to the indicated proteins. **E.** Long term viability assay of MGH156-1A cells. Cell were treated with vehicle, gefitinib (1.0 μM), BGJ-398 (1.0 μM) or the combination of both drugs for 7 days. The plates were then stained with crystal violet.

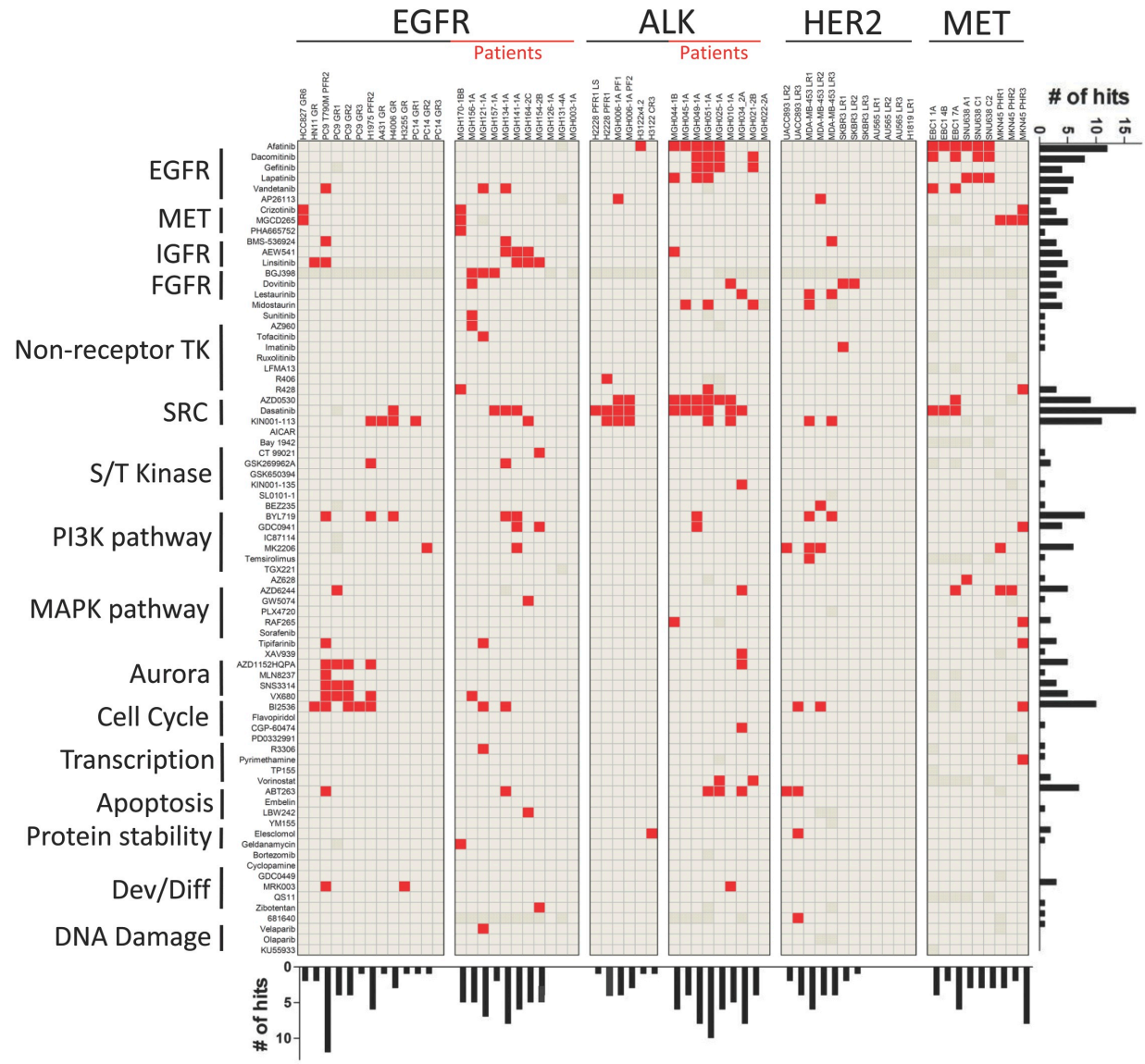

Fig. S5: Representation of all screen hits. Each hit is represented as a red box. All other model-drug combinations are represented in beige. The absence of data is indicated by darker beige. Each column represents a cell line model (labeled). EGFR, ALK, HER and MET lines are segregated. Additionally, patient-derived models are presented separately from *in vitro*-derived lines. Each row represents a drug (labeled), and drugs targeting the same target, pathway or mechanism are clustered as labeled. Bar graphs represent the number of hits for each drug (along the y-axis) and each cell line (along the x-axis).

ALK (patient derived)

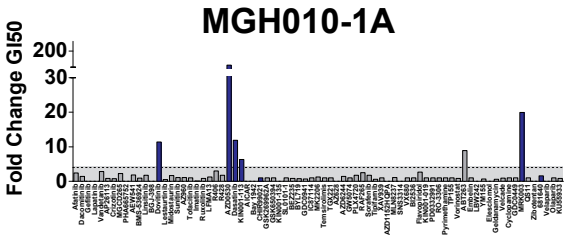

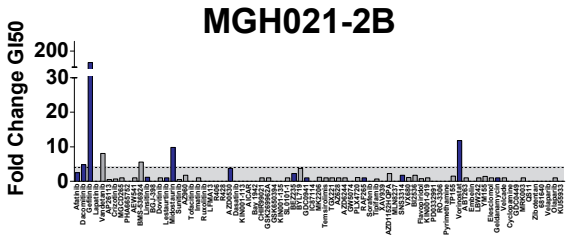

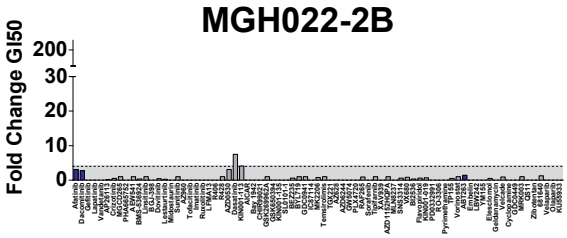

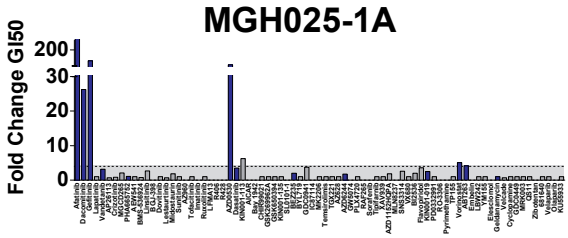

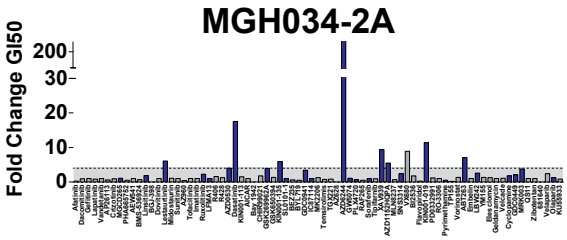

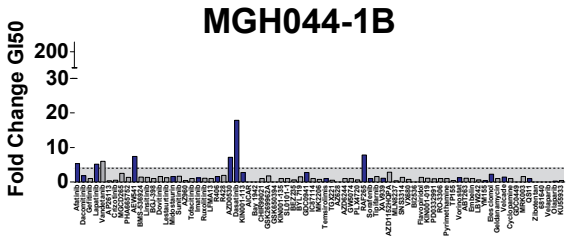

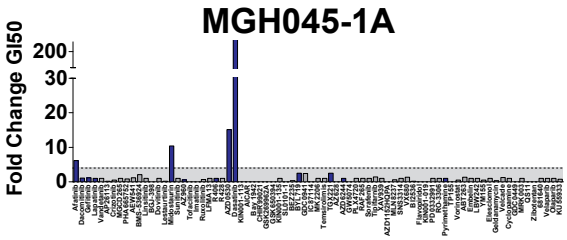

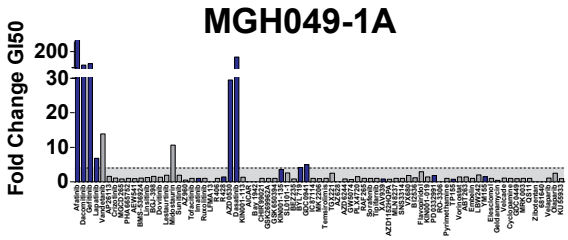

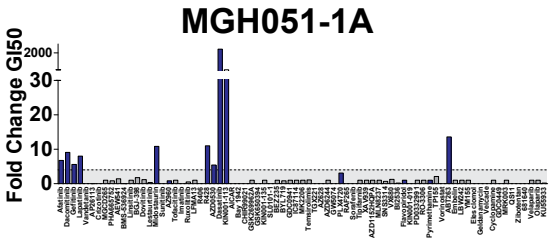

Fig. S6

EGFR (patient derived)

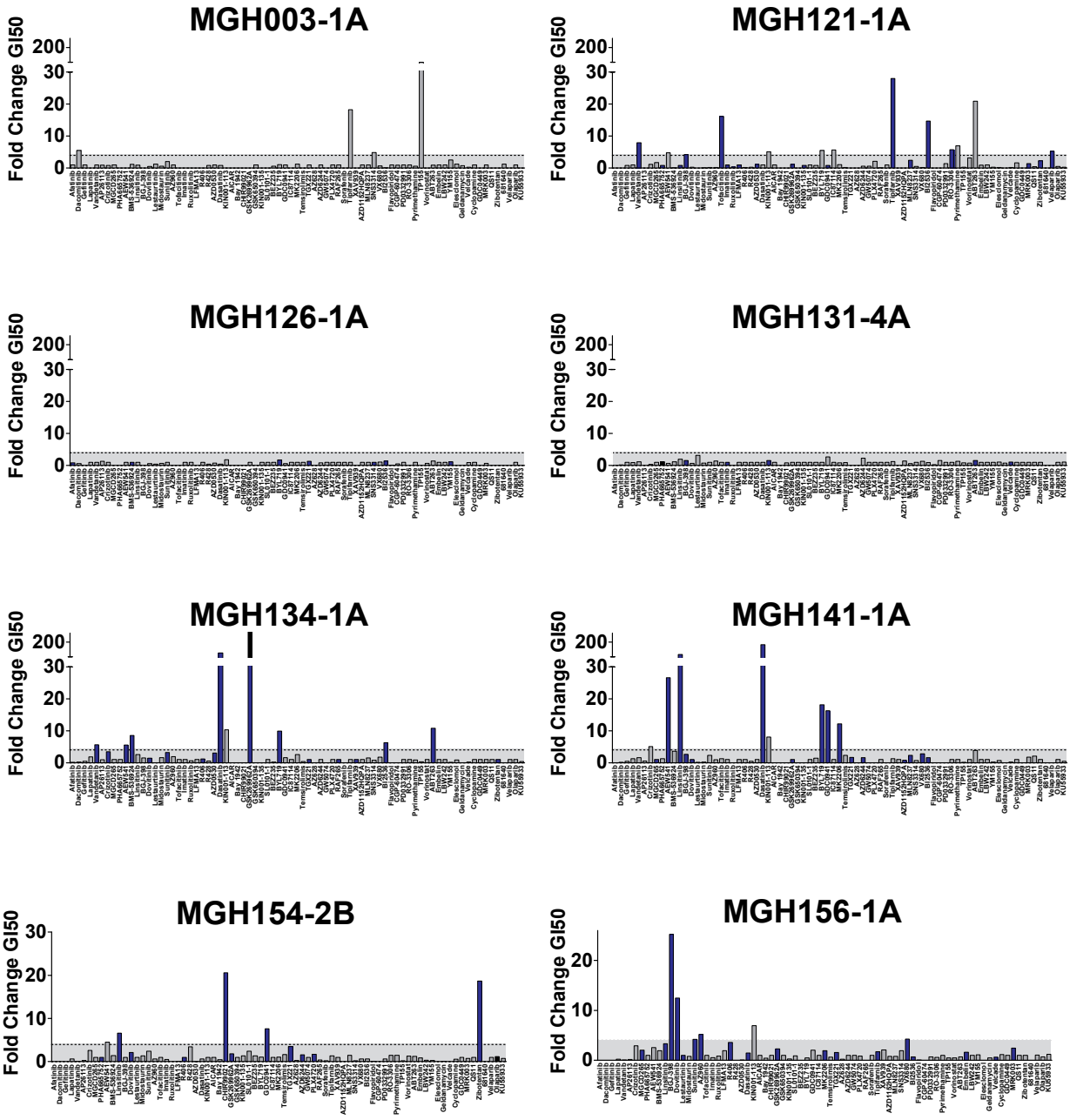

Fig. S6 (cont)

EGFR (patient derived)

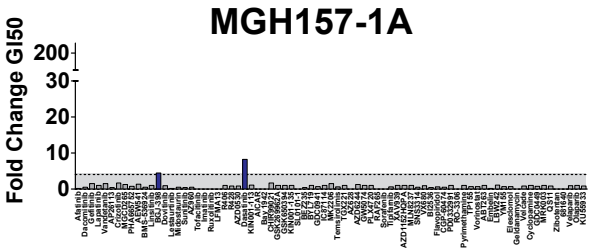

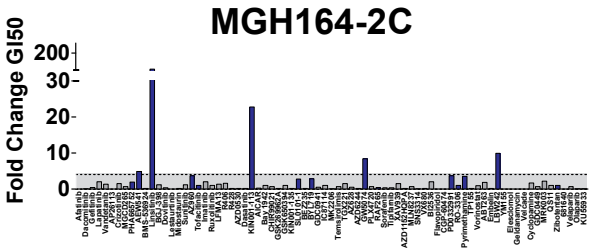

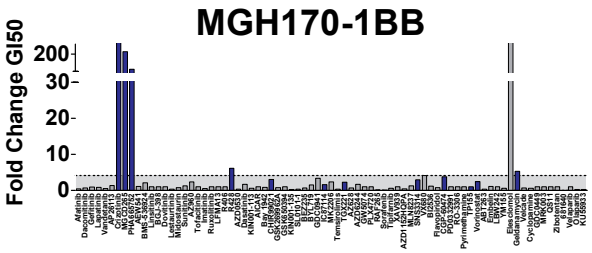

Fig. S6 (cont)

ALK (in vitro)

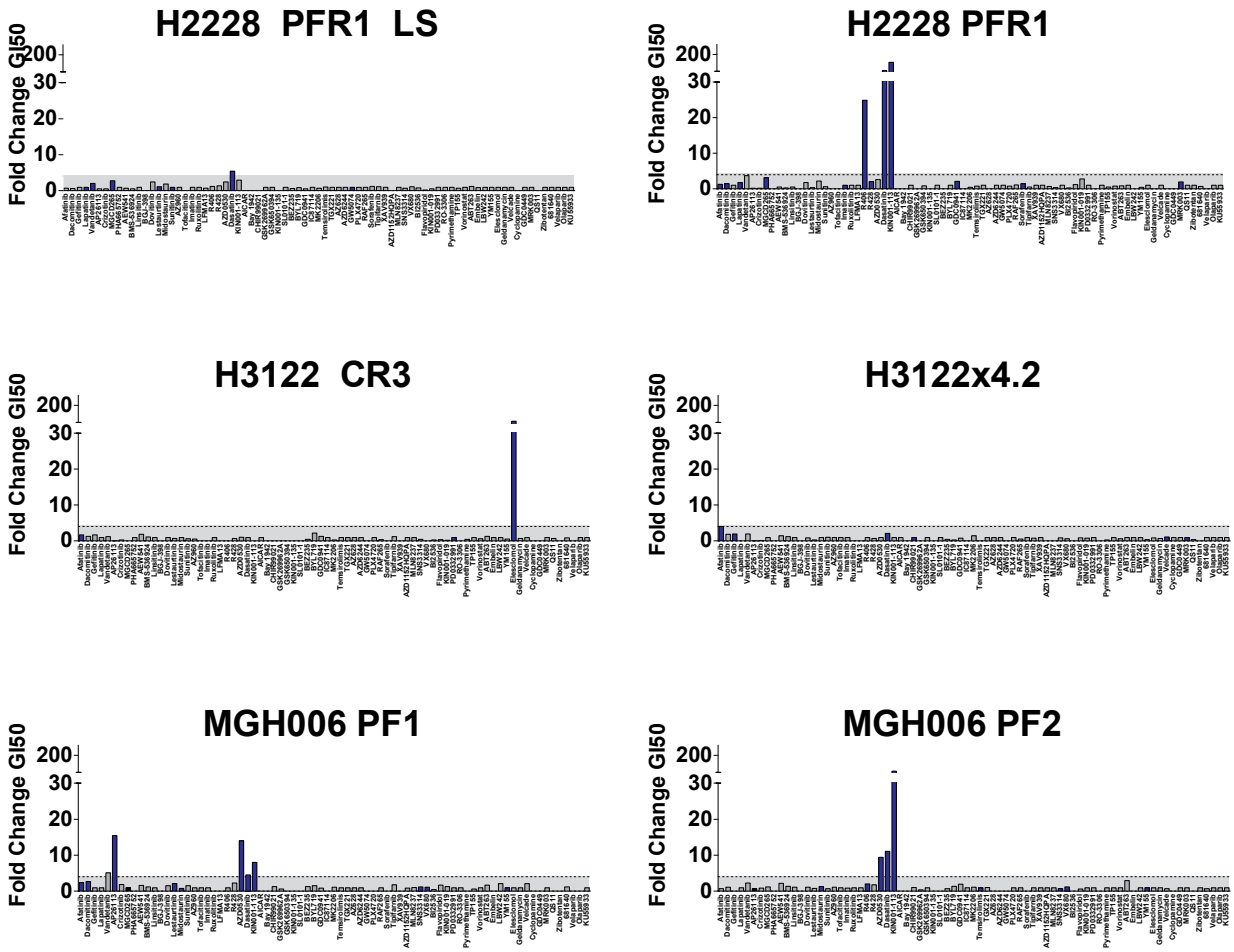

Fig. S6 (cont)

EGFR (in vitro)

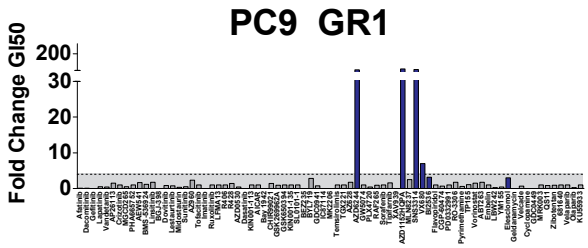

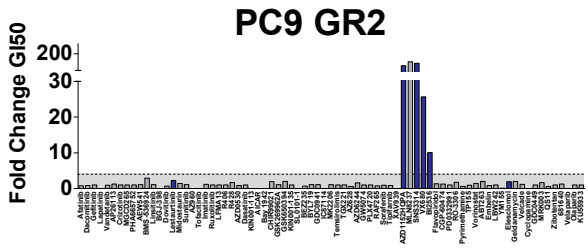

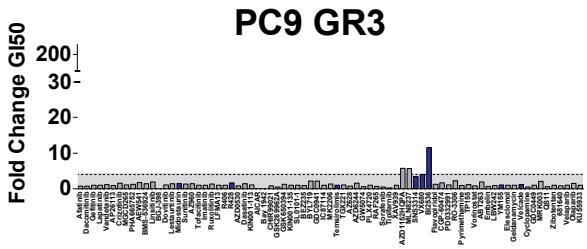

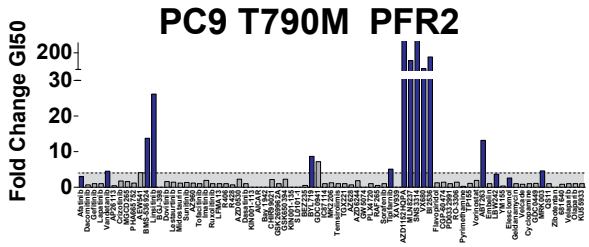

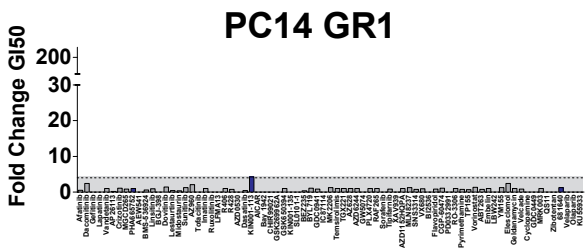

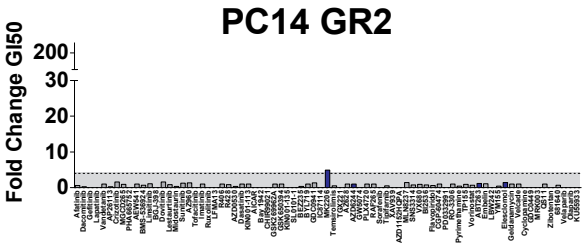

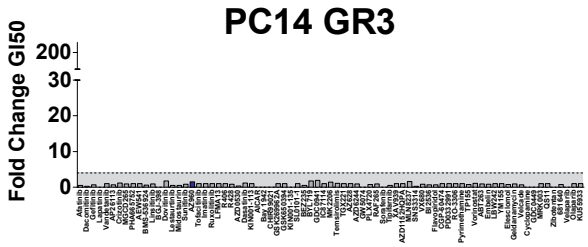

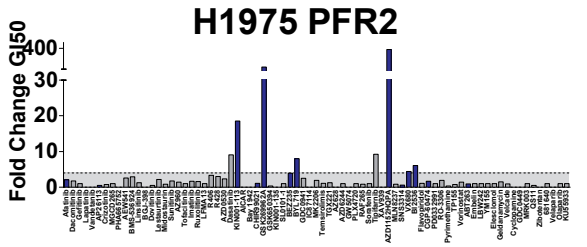

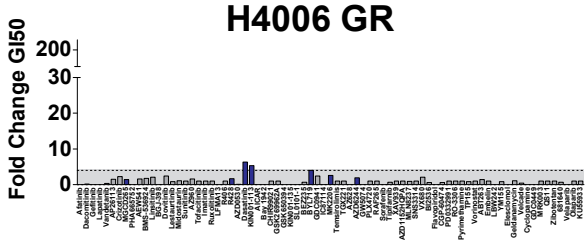

Fig. S6 (cont)

EGFR (in vitro)

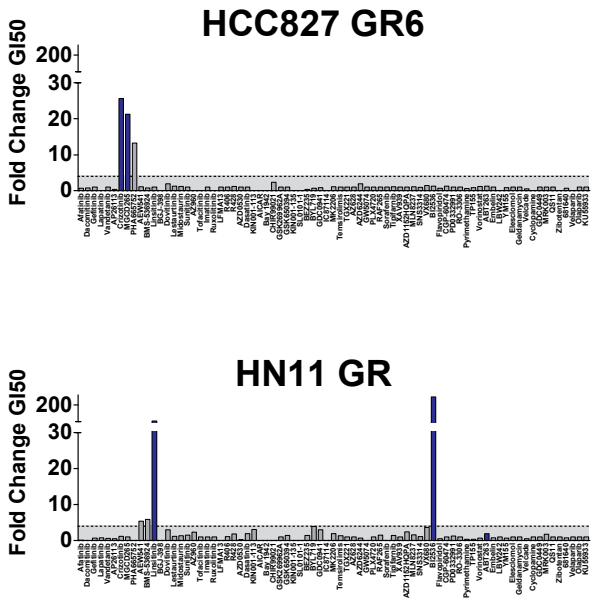

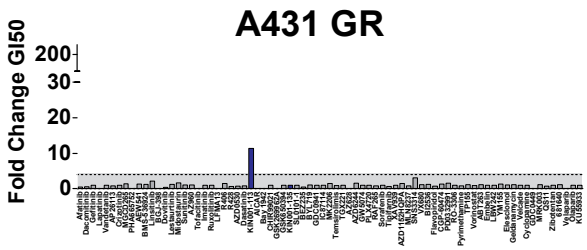

Fig. S6 (cont)

HER2 (in vitro)

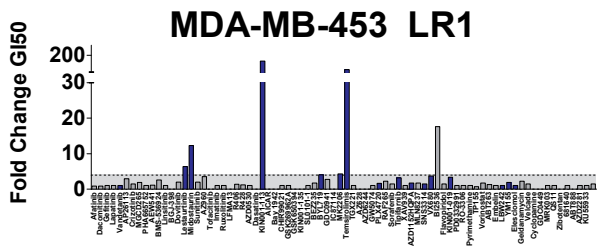

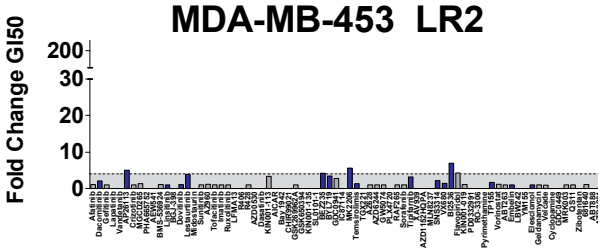

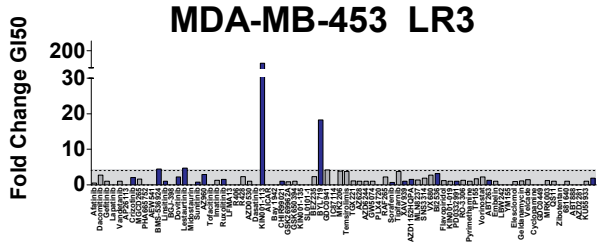

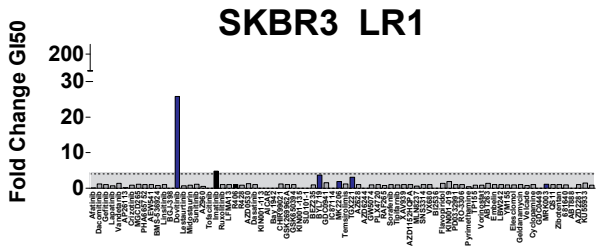

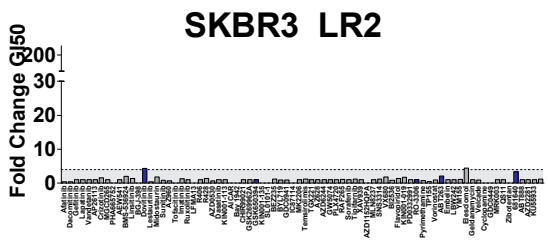

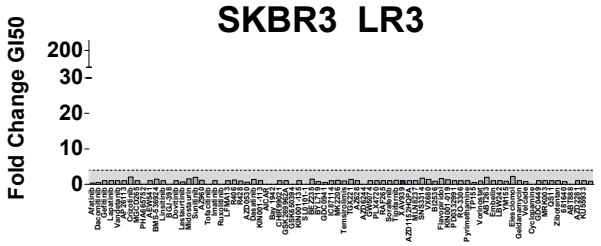

Fig. S6 (cont)

HER2 (in vitro)

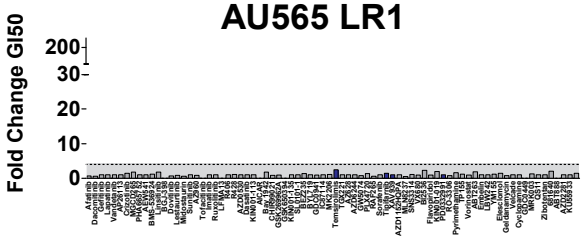

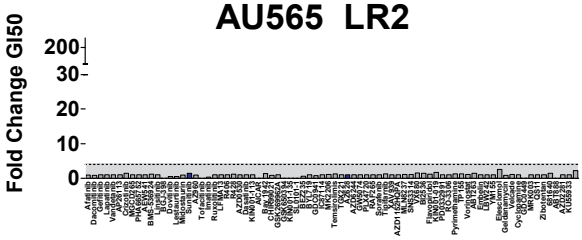

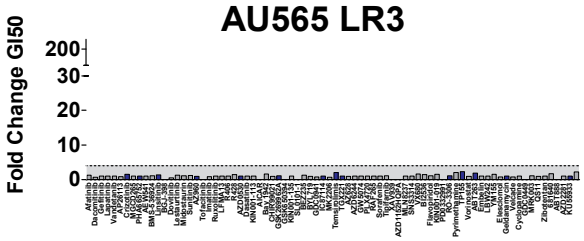

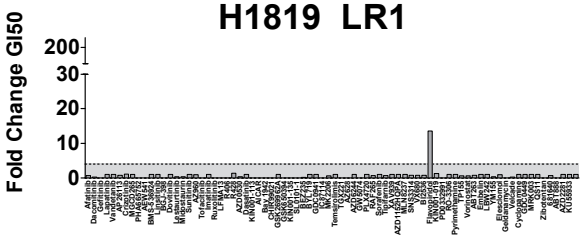

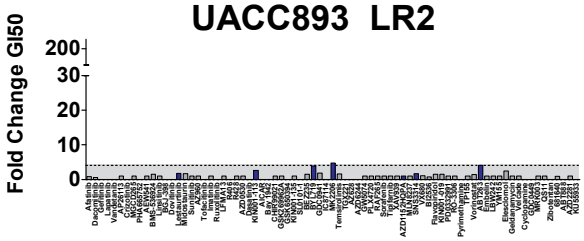

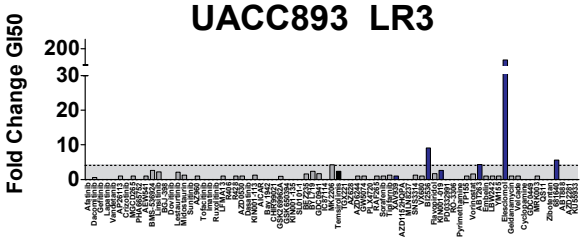

Fig. S6 (cont)

MET (in vitro)

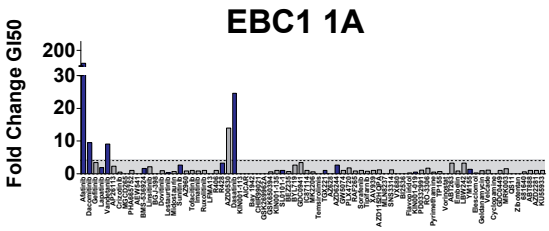

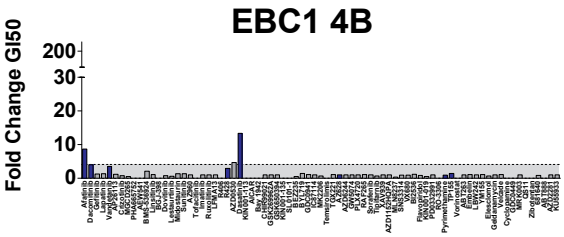

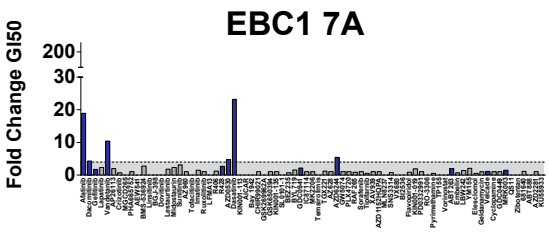

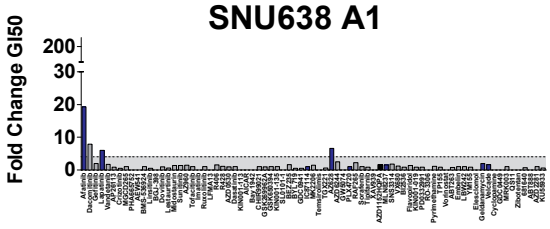

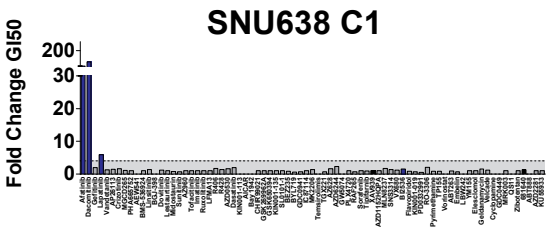

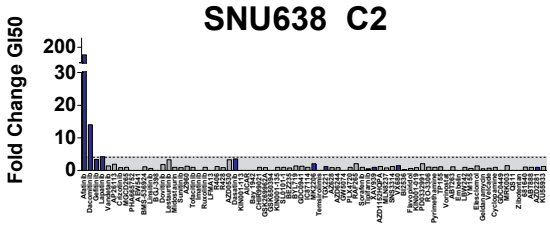

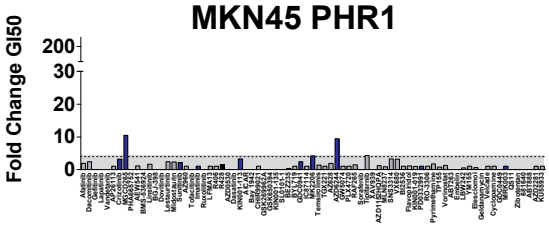

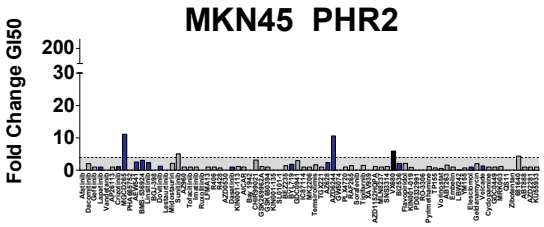

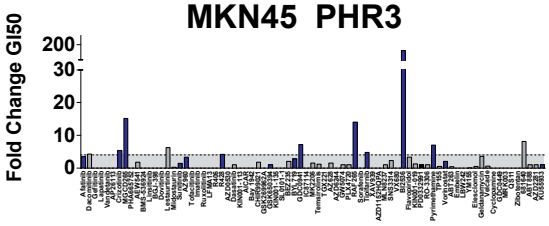

Fig. S6 (cont)

Fig. S6: Representation of the hits for each cell line. In each graph the fold-change in GI50 is represented on the y-axis. Each column represents one drug (labeled). Those drugs that achieved a change in AUC>10% are represented in blue. Those with change in AUC<10% are represented in grey. Hits are those drugs with both AUC>10% and fold-change GI50>4.

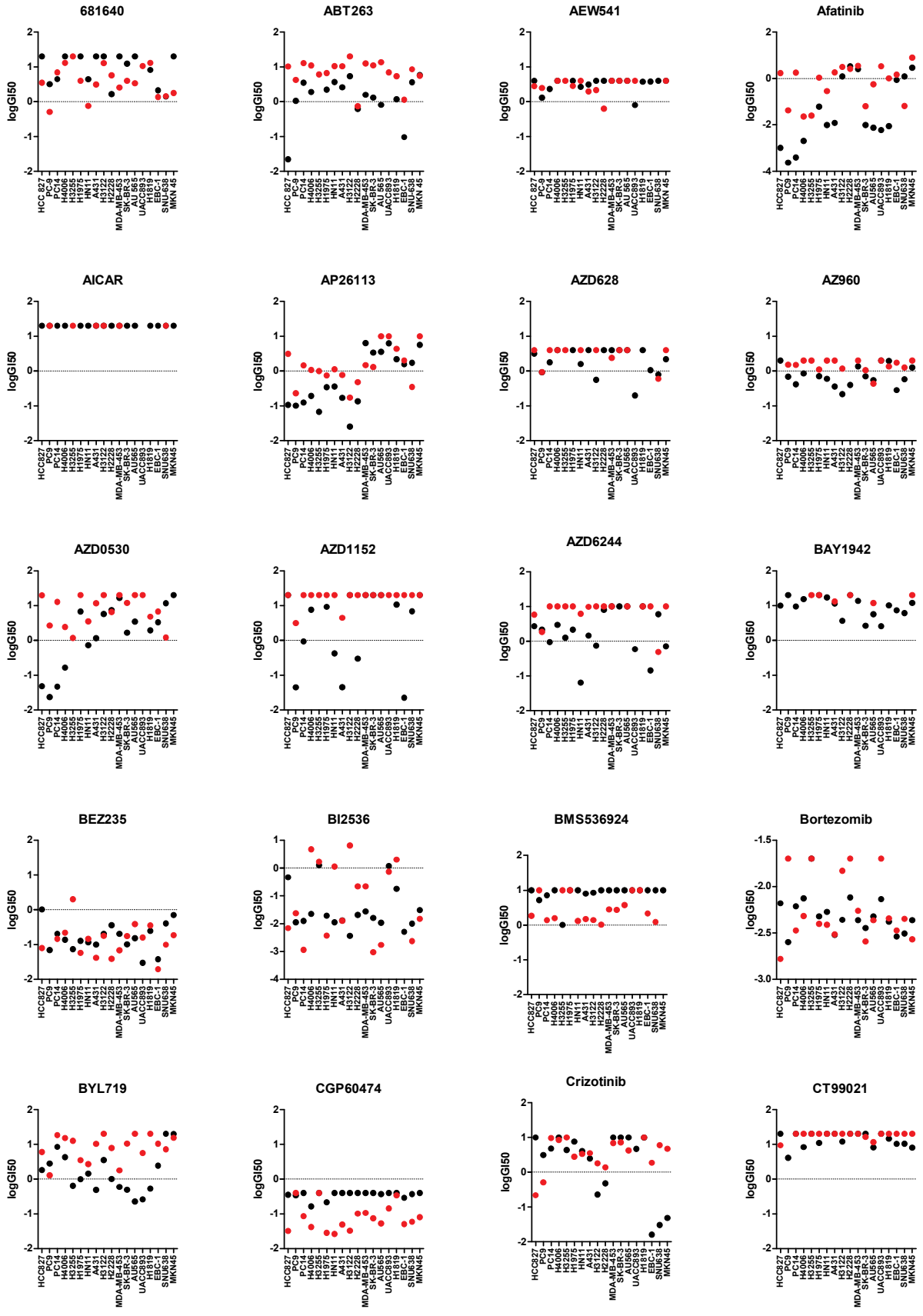
681640
ABT263
AEW541
Afatinib
AICAR
AP26113
AZD628
AZ960
AZD0530
AZD1152
AZD6244
BAY1942
BEZ235
BI2536
BMS536924
Bortezomib
BYL719
CGP60474
Crizotinib
CT99021
logGI50

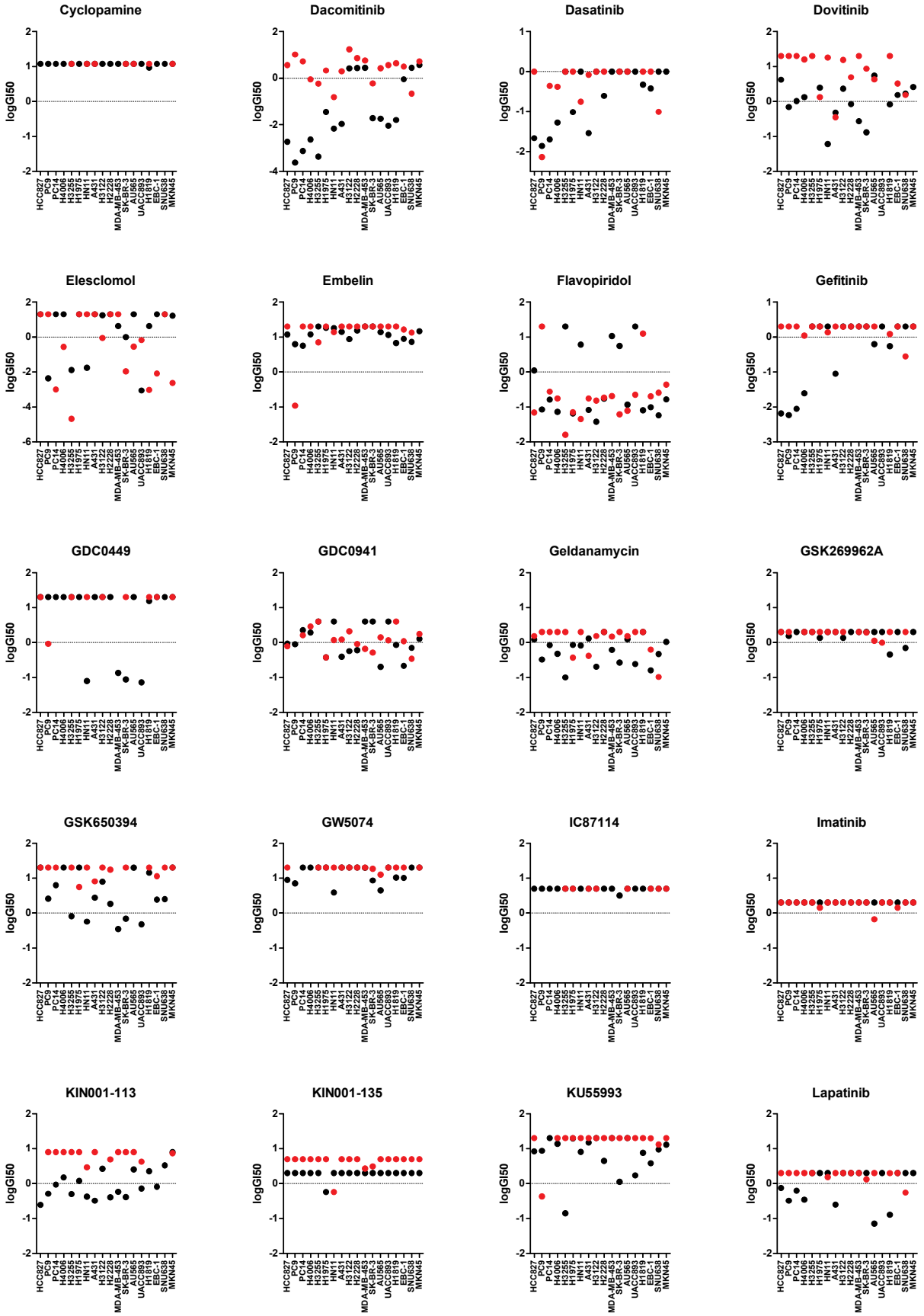
Cyclopamine
Dacomitinib
Dasatinib
Dovitinib
Elesclomol
Embelin
Flavopiridol
Gefitinib
GDC0449
GDC0941
Geldanamycin
GSK269962A
GSK650394
GW5074
IC87114
Imatinib
KIN001-113
KIN001-135
KU55993
Lapatinib
logGI50
HCC827 PC9 PC14 H4006 H3255 H1975 HN11 A431 H3122 H2228 MDA-MB-453 SK-BR-3 AU565 UACC893 H1819 EBC-1 SNU638 MKN45

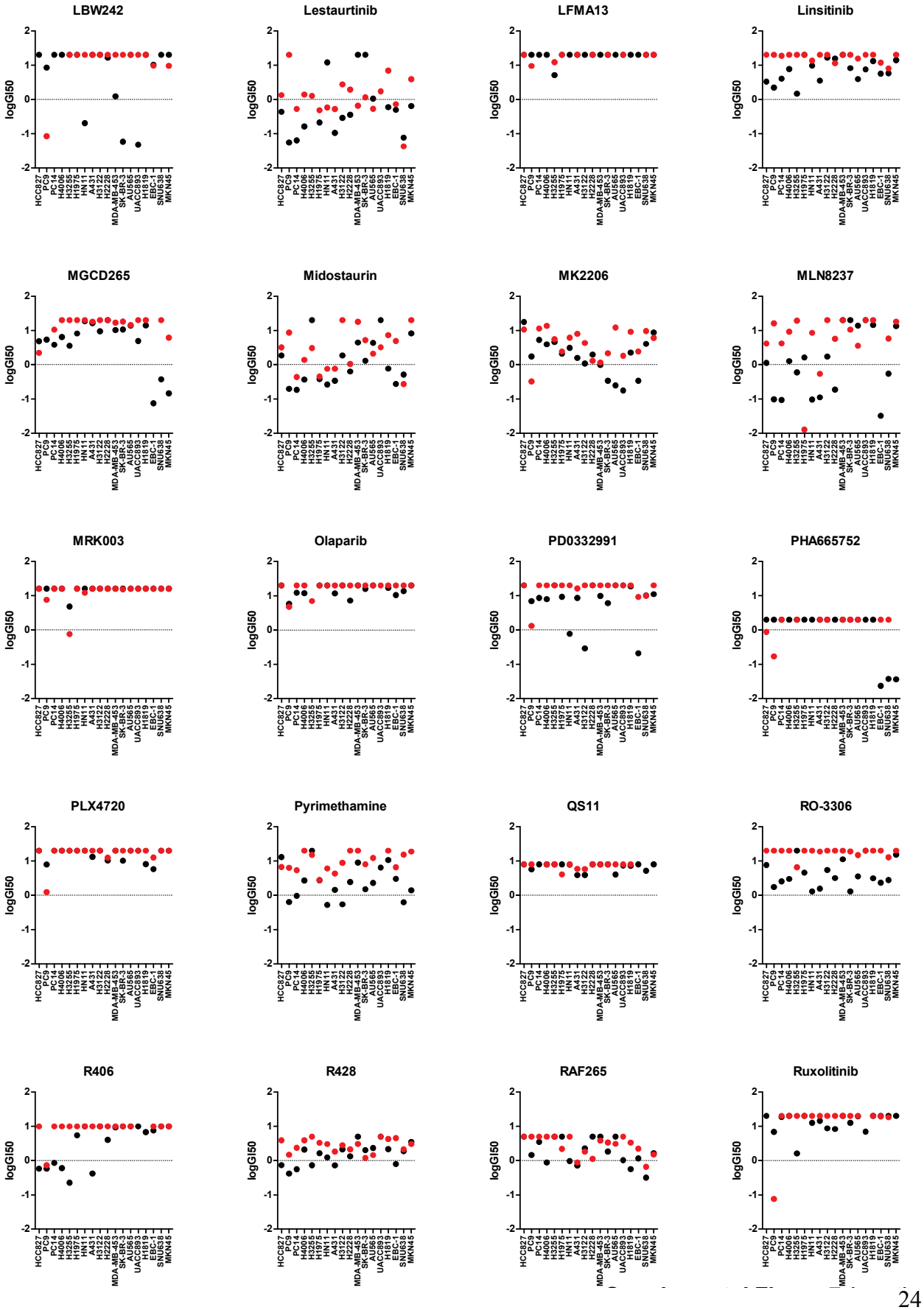
LBW242
Lestaurtinib
LFMA13
Linsitinib
MGCD265
Midostaurin
MK2206
MLN8237
MRK003
Olaparib
PD0332991
PHA665752
PLX4720
Pyrimethamine
QS11
RO-3306
R406
R428
RAF265
Ruxolitinib
logGI50
2
1
0
-1
-2
HCC827
PC9
PC14
H4006
H3255
H1975
HN11
A431
H3122
H2228
MDA-MB-453
SK-BR-3
AU565
UACC893
H1819
EBC-1
SNU638
MKN45

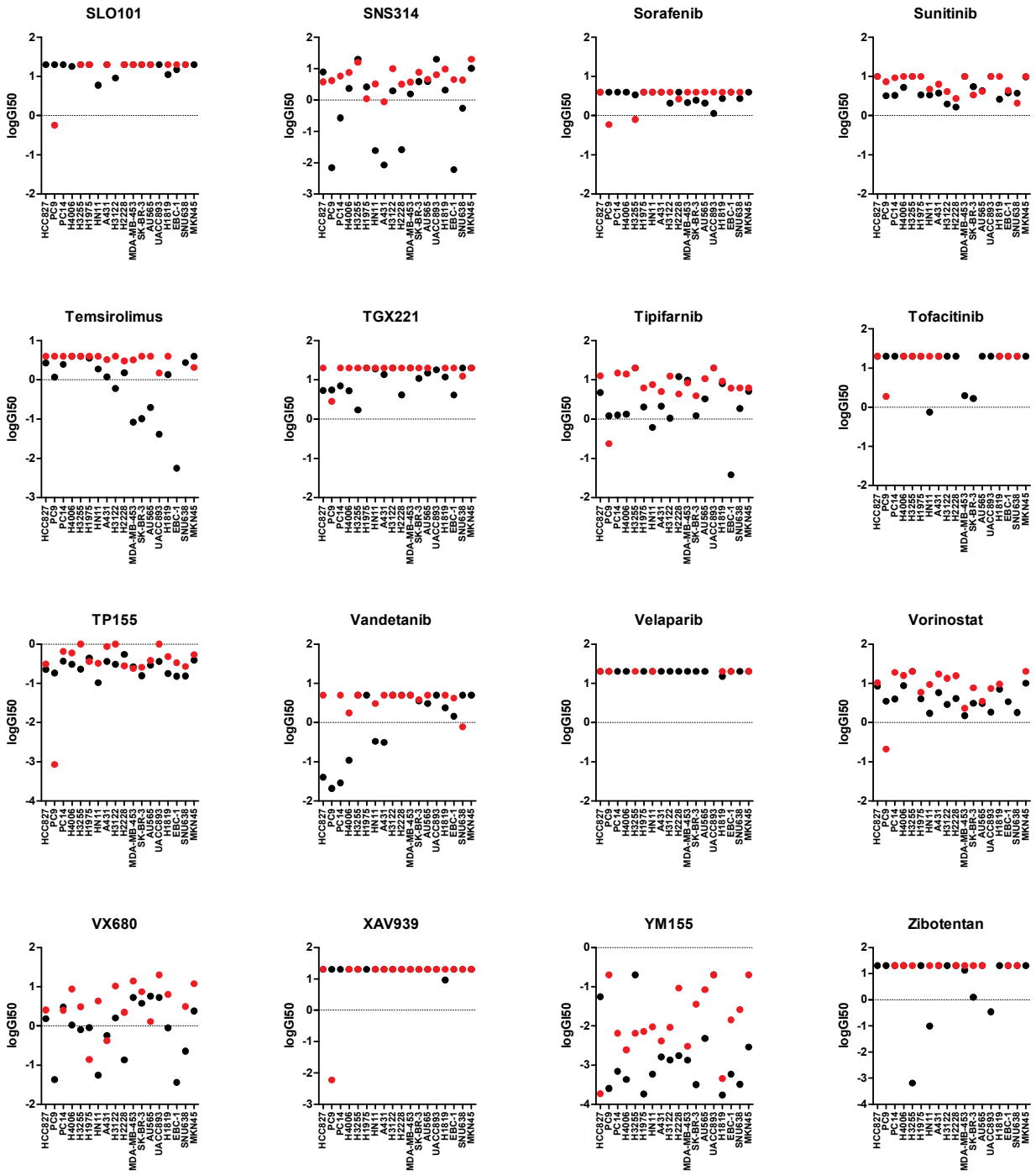

Fig. S7: Comparison of GI50 for screen compounds in parental cell lines and the acquired resistance model derived from each line. Each screen compound is presented in a separate graph. On each graph the y-axis represents the log(GI50) of the indicated compound. Each parental/resistance model is presented on a single column. The parental line is represented in black and the resistant model in red.

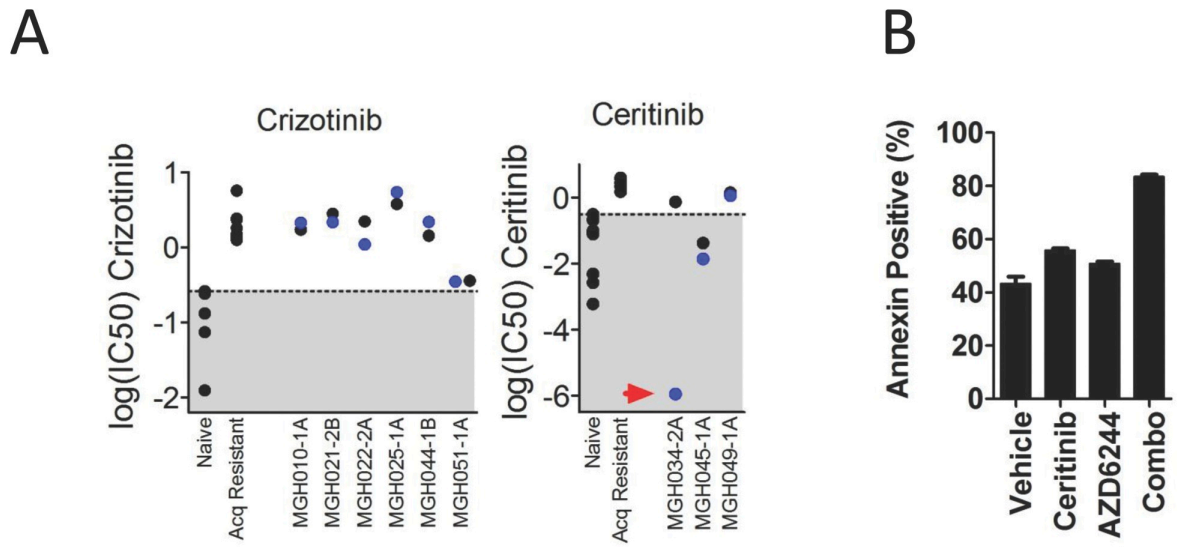

Fig. S8: AZD6244 re-sensitizes MGH034-2A to ceritinib. A. The GI50 of each ALK-positive resistant patient-derived model to single-agent crizotinib or ceritinib (represented by black dots) or in combination with AZD6244 1 μM (represented by blue dots) is shown. Models of sensitivity (MGH006-1A, H3122, SU-DHL-1, KARPAS299, NB-1) and acquired resistance (MGH006-1A PFR1, MGH006-1A PFR2, H2228 PFR1, H3122 PFR1, H3122 PFR3, H3122 x4.2) to crizotinib are presented as standards for comparison (*34*). Models of sensitivity (H3122, H2228, MGH051-1, H3122 PFR2, MGH021-2cl4, MGH006-1A, MGH026-1A, MGH039-1A) and acquired resistance (MGH021-5A, H3122 LDKR1, H3122 LDKR2, H3122 LDKR3, H3122 LDRK4) to ceritinib are presented as standards for comparison. The mean GI50 of three independent experiments is presented. The shaded area indicates the region typical of sensitive lines. **B.** MGH034-2A cells were treated with vehicle, ceritinib (0.3 μM), AZD6244 (1 μM) or the combination of both drugs for 72 hours, and apoptosis was assessed by measuring annexin positivity.

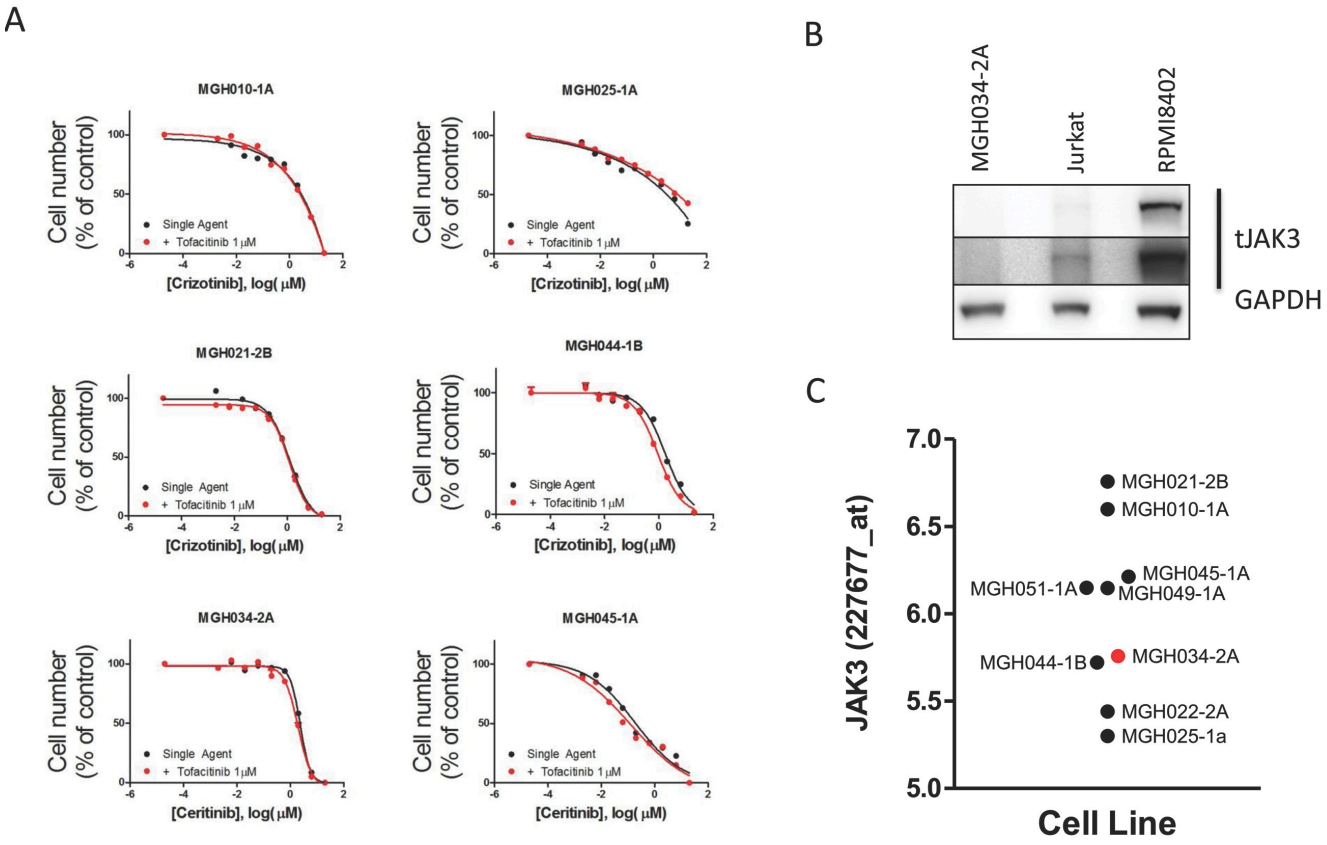

Fig S9: JAK3 does not likely promote resistance to ALK inhibition. A. A dose-response demonstrating the effect of JAK3 inhibition with tofacitinib (1 μM) on sensitivity to the indicated ALK inhibitor is shown. Each point done in triplicate. Error bars are mean -/+ SEM. **B.** Western blot analysis of cell lysates from MGH034-2A, Jurkat and RPMI8402 cells. Lysates were blotted with antibody to the indicated proteins. Two exposures of the tJAK3 Western blot are presented. **C.** Relative JAK3 gene expression for each of the patient derived ALK lines is presented.

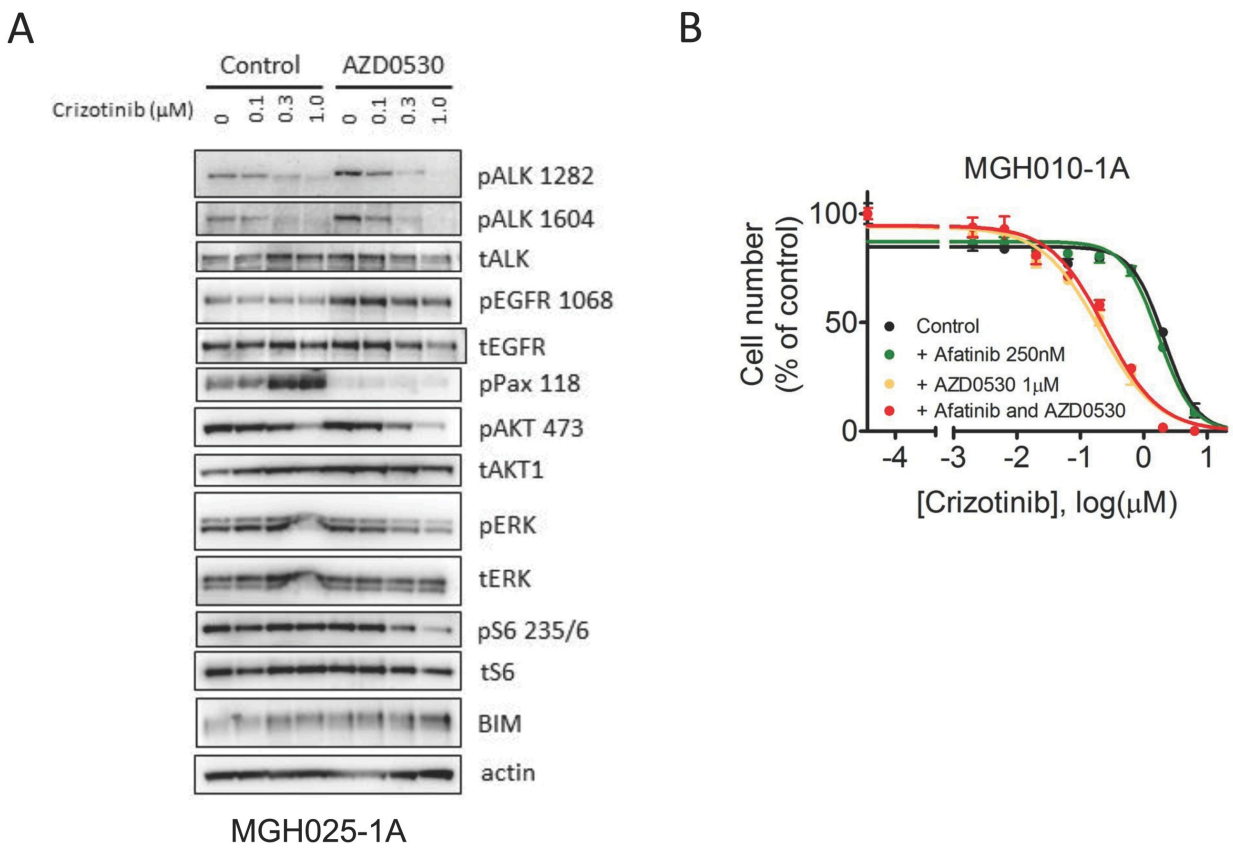

Fig. S10: The efficacy of AZD0530 is not due to inhibition of EGFR. A. Western blot analysis of MGH025-1A cells. Cells were treated with increasing concentrations of crizotinib (0, 0.1 μM, 0.3 μM, 1.0 μM) as single-agent or in the presence of AZD0530 (1 μM) for 24 hours. Lysates were prepared and subject to analysis with antibodies to the indicated proteins. **B.** Dose-responses to crizotinib are presented in a patient-derived ALK model of acquired resistance to crizotinib, MGH010-1A. Crizotinib was tested as single agent (black), with 250 nM afatinib (green), with 1 μM AZD0530 (orange) or with both AZD0530 and afatinib (red). The best-fit line represents the variable slope: log(inhibitor) vs. response. After 72 hours of drug treatment cell counts were determined using CellTiter-Glo. Each point was done in triplicate. Error bars are mean -/+ SEM. The experiment was repeated 3 times and a representative result is presented.

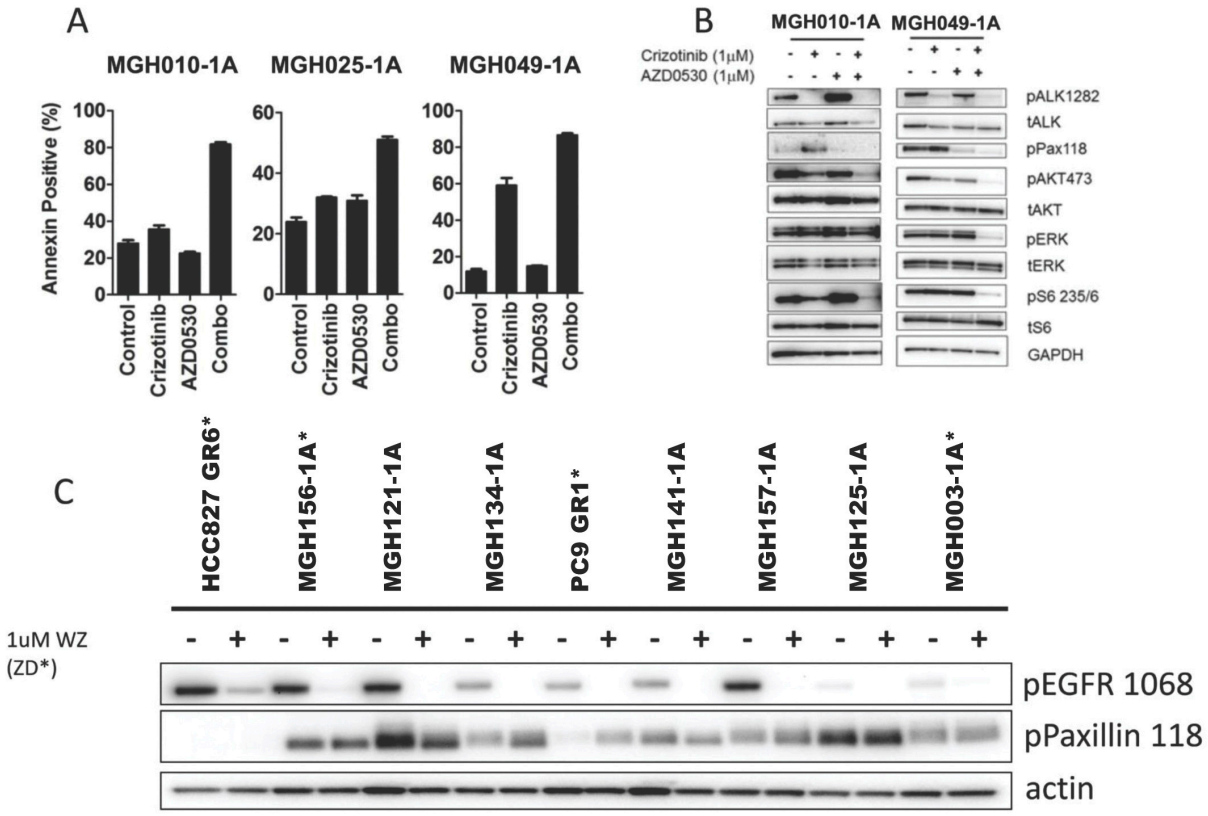

Fig. S11: Combined ALK and SRC inhibition induces apoptosis and suppresses signaling. **A.** MGH010-1A, MGH025-1A and MGH049-1A cells were treated with vehicle, crizotinib (1 μM), AZD0530 (1 μM) or the combination of both drugs for 72 hours then subjected to PI and annexin staining and flow cytometric analysis. The y-axis represents the percentage of cells under each condition that were positive for annexin staining. Each point was done in triplicate. The experiment was repeated 3 times and a representative result is presented. **B.** Western blot analysis of MGH010-1A and MGH049-1A cells. Cells were treated with crizotinib (1 μM), AZD0530 (1 μM) or the combination for 24 hours. Lysates were prepared and subject to analysis with antibodies to the indicated proteins. **C.** Western blot analysis of resistant EGFR mutant lung cancer models demonstrates that p-Paxillin is not consistently upregulated by EGFR inhibition. Lysates were prepared after 24 hours of drug treatment and blotted with antibodies directed against the indicated proteins.

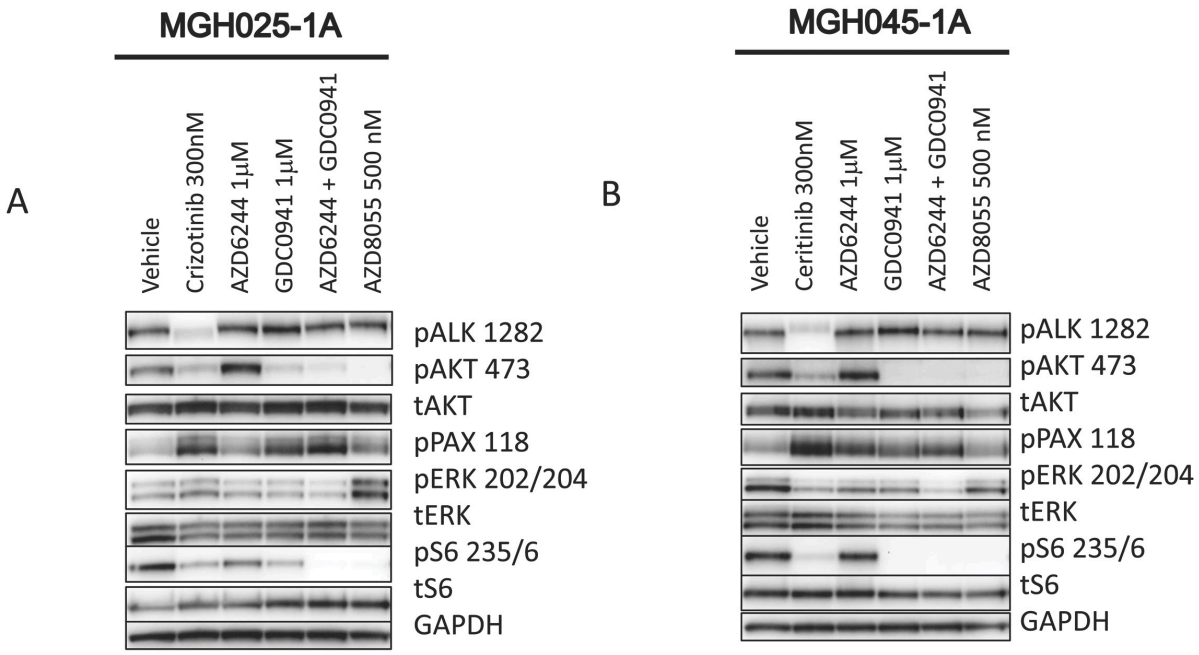

Fig. S12: The feedback on SRC signaling is downstream from ALK. A. MGH025-1A were treated for 24 hours with the indicated compound and lysates were prepared then blotted with antibody directed against the indicated proteins. **B.** MGH045-1A were treated for 24 hours with the indicated compound and lysates were prepared then blotted with antibody directed against the indicated proteins.

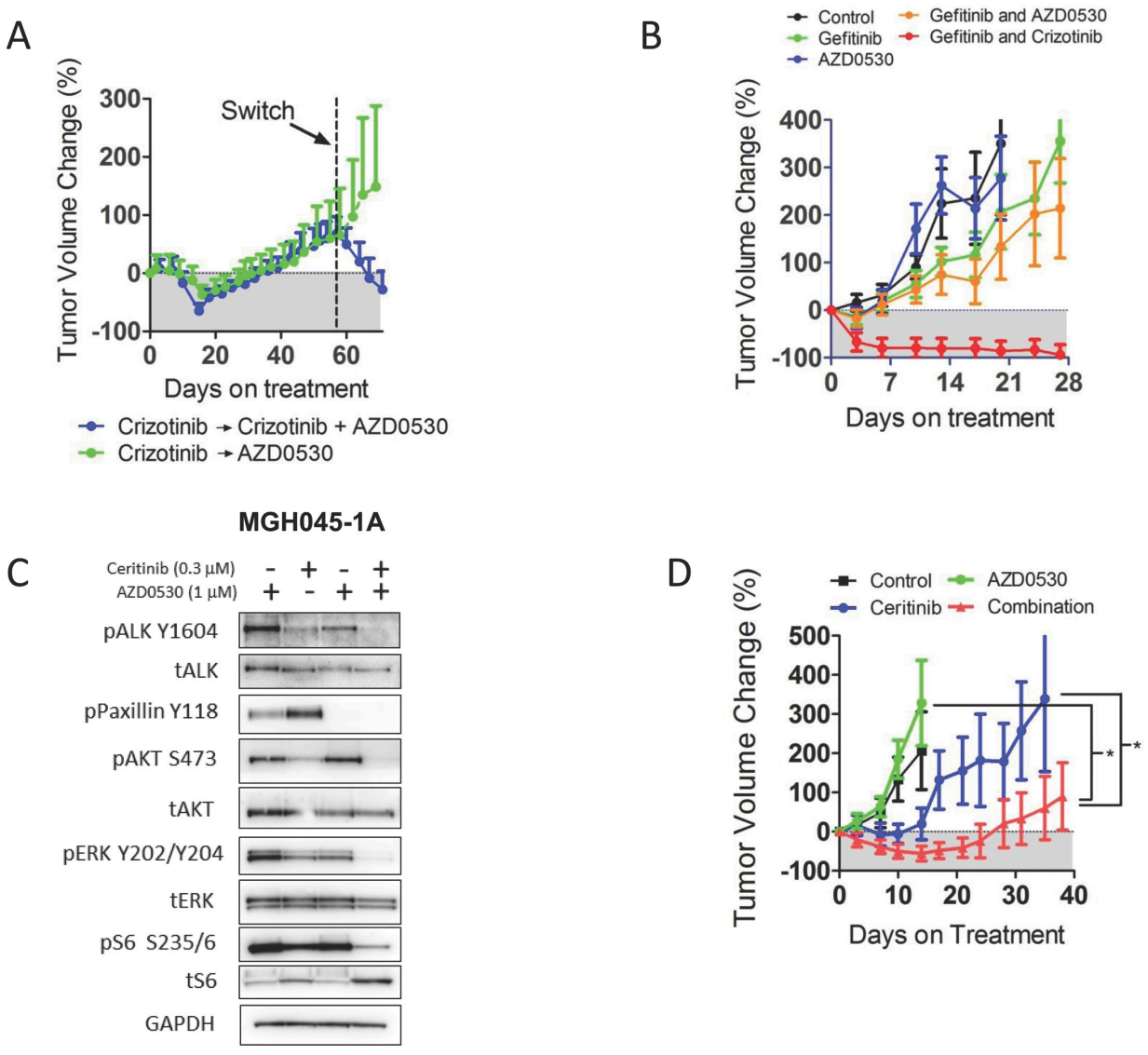

Fig. S13: The combination of ALK inhibition and AZD0530 is effective in vivo against ALK inhibitor resistant cells as well as in a model sensitive to the ALK inhibitor ceritinib. A. The crizotinib treatment arm of the MGH025-1A xenograft experiment (Fig. 5D) was divided into two groups of 3 mice each. After treatment was held for 3 days, one group was switched to AZD0530 (50 mg/kg daily) (green) and the other was treated with crizotinib (25 mg/kg daily) plus AZD0530 (50 mg/kg daily) (blue). Bars represent SEM. **B.** HCC827 GR6 xenografts were divided into 5 treatment arms: Control (black, n=4), gefitinib (green, n=5), AZD0530 (blue, n=4), gefitinib and AZD0530 (orange, n=4) or gefitinib and crizotinib (red, n=5). **C.** Western blot analysis of MGH045-1A. In this experiment cells were treated with vehicle, ceritinib (300 nM), AZD0530 (1 μM) or the combination of both drugs for 24 hours. Lysates analyzed with antibodies to the indicated proteins. **D.** Using the partially ceritinib sensitive MGH045-1A subcutanous xenografts were generated and treated as indicated: Control (n=6), ceritinib 25 mg/kg daily (n=6), AZD0530 50 mg/kg daily (n=6), or the combination of both (n=6). Error bars are mean -/+ SEM. Asterisks indicate $P<0.0001$ by Dunn's Multiple Comparison Test.

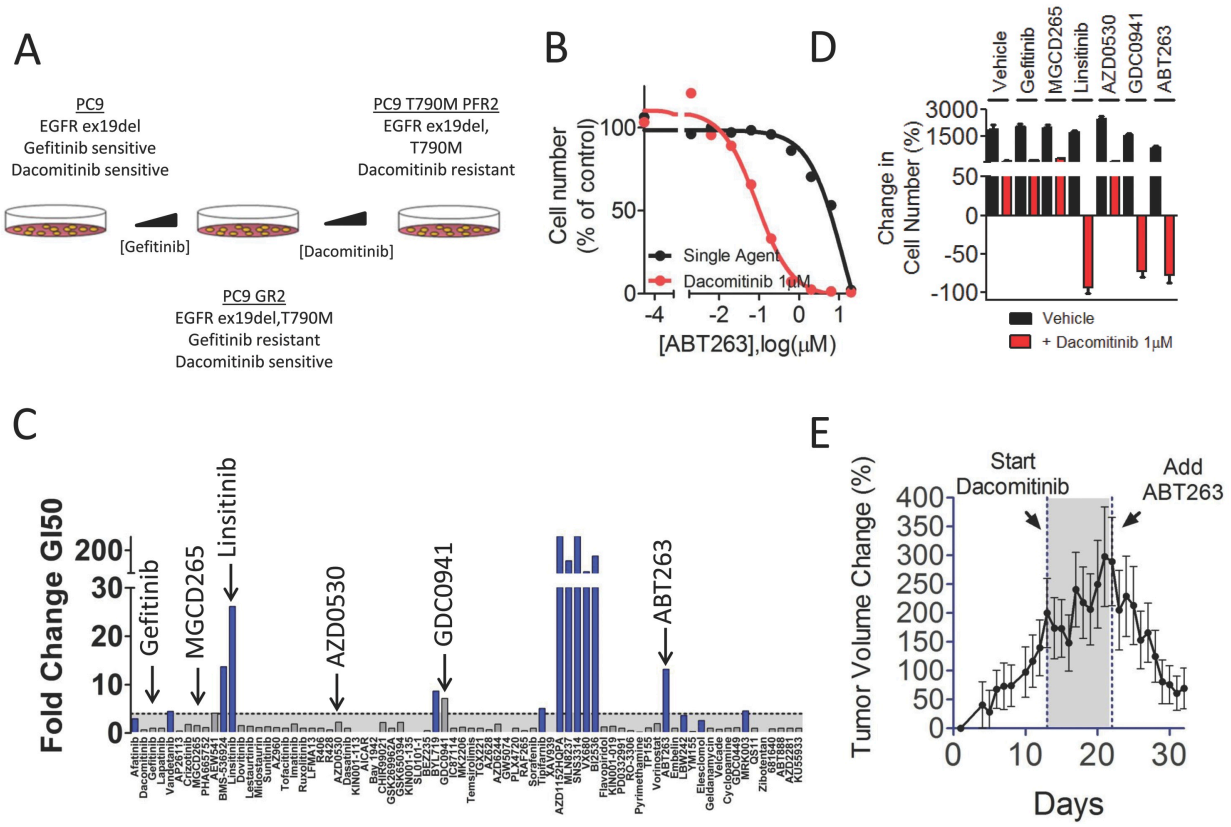

Figure S14: The combination of dacominitib and ABT263, observed as a hit in PC9 T790M PFR2 (EGFR T790M model resistant to dacomitinib) is effective *in vivo*. A. Schematic representing the derivation of model PC9 T790M PFR2. **B.** Primary screen data in the model PC9 T790M PFR2. The dose-response to AT263 is presented both as single agent (black) and in the presence of dacominitinb (red). The best-fit line represents the variable slope [log(inhibitor) vs. response]. **C.** Representation of screen data for all compounds tested against PC9 T790M PFR2. The y-axis represents the Fold-change GI50 that results with the addition of dacomitinib. The bars are color-coded blue when the percent decrease in AUC from single agent to combination is greater than 10%. Drugs represented in panel D are highlighted with arrows. **D.** Viability assay of PC9 T790M PFR2 demonstrating the percentage change in cell number in comparison to cell count at initiation of treatment (y-axis) after 6 days of treatment with vehicle, dacomitinib (1 μM), single agent gefitinib (1 μM), MGCD265 (1 μM), OSI906 (1 μM), AZD0530 (1 μM), GDC0941 (250 nM) and ABT263 (1 μM) (black) and the combination of each drug with dacomitinib (red). This data was generated in the experiment to determine hit threshold (Fig. S12). **E.** Subcutaneous xenografts of PC9 T790M PFR2 were used to assess *in vivo* efficacy of combination treatment by measuring change in tumor volume. Thirteen days after cell injection, treatment was initiated with dacomitinib (10 mg/kg daily). After tumors progressed on dacomitinib (day 22), ABT263 (100 mg/kg daily) was added to the treatment regimen.

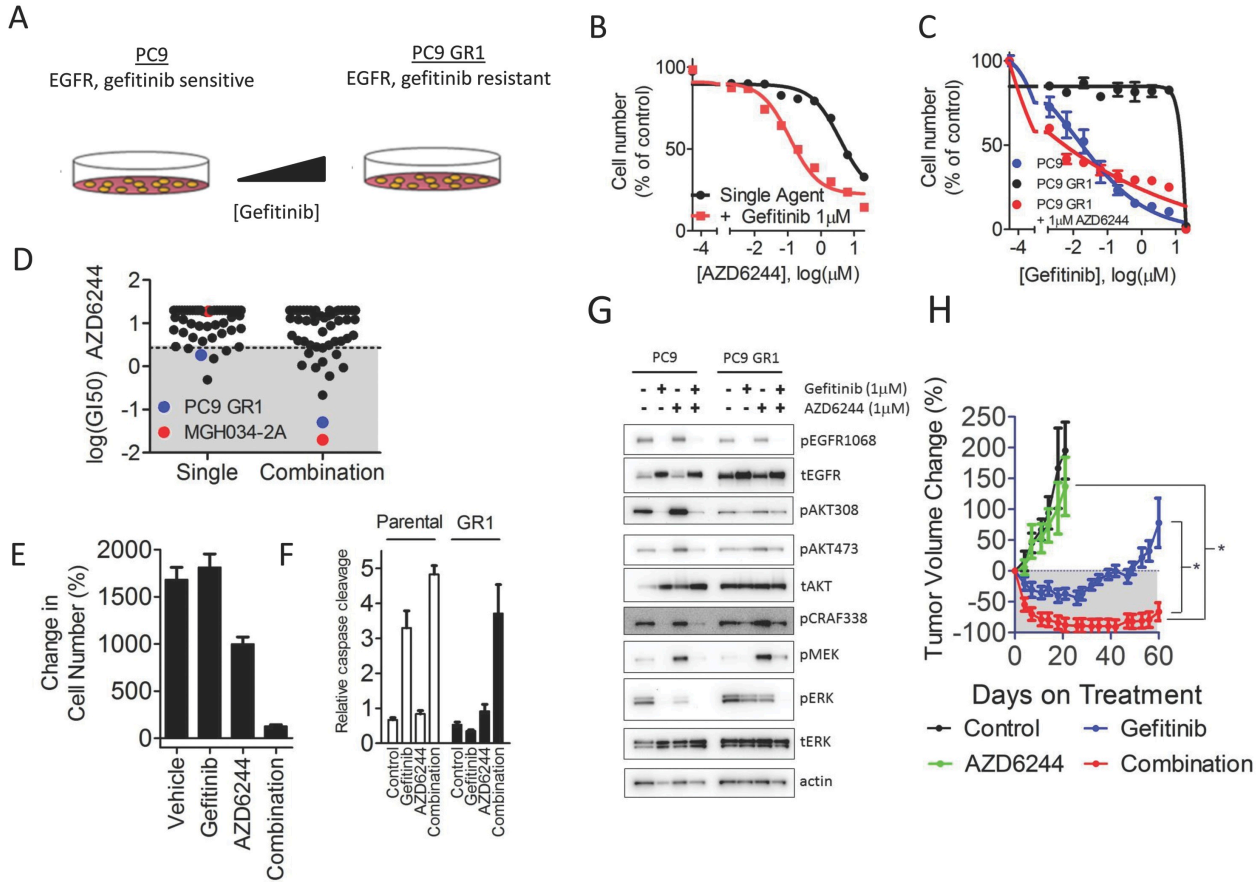

Figure S15: AZD6244 is effective in the PC9 GR1 model. A. Schematic representation of the derivation of the model PC9 GR1 (EGFR-mutant NSCLC line with *in vitro*-derived resistance to gefitinib). **B.** Primary screen data demonstrating the dose-response curve to AZD6244 of PC9 GR1 in the presence (red) or absence (black) of gefitinib (1 μM). The best-fit line represents the variable slope: log(inhibitor) vs. response. After 72 hours of drug treatment cell counts were determined using CellTiter-Glo. Please see Fig. S6 for complete results of the screen on this cell line. **C**. Dose-response demonstrating the effect of MEK inhibition with AZD6244 (1 μM) on sensitivity to gefitinib. The best-fit line represents the variable slope: log(inhibitor) vs. response. After 72 hours of drug treatment cell counts were determined using CellTiter-Glo. Each point done in triplicate. Error bars are mean -/+ SEM. The experiment was repeated 3 times, and a representative result is presented. **D.** Comparison of AZD6244 potency across all screened lines when administered as single agent or combination. The values for PC9 GR1 are presented in green, and the values for MGH034-2A in red. **E.** Viability assay of PC9 GR1 cells demonstrating the percentage change in cell number (y-axis) after 6 days of treatment with vehicle, gefitinib (1 μM), AZD6244 (1 μM) or the combination of both drugs in comparison to the number of cells at the initiation of drug exposure (five replicates). The error bars are mean -/+ SEM. **F.** Determination of apoptosis as measured by increase in caspase 3/7 cleavage in both PC9 parental and PC9 GR1 cells. Cells were plated in 5 replicates in a 96-well format and treated for 48 hours with vehicle, gefitinib (1 μM), AZD6244 (1 μM) or the combination of both drugs. Caspase

activity was then quantified with CaspaseGlo 3/7 (Promega). The experiment was repeated 3 times and a representative example is presented. The error bars are -/+ SEM**. G.** Cells were treated with vehicle, gefitinib (1 μM), AZD6244 (1 μM) or the combination of both drugs for 24 hours. Lysates were prepared and subject to analysis with antibodies to the indicated proteins. **H.** Subcutaneous xenografts of PC9 GR1 were generated and treated as indicated: Control (n=6), gefitinib 35 mg/kg daily (n=6), AZD6244 25 mg/kg BID (n=6), or the combination of both (n=6). The y-axis represents the change in tumor size from the initiation of drug treatment. Error bars are mean -/+ SEM. Asterisks indicate $P<0.05$ by Dunn's Multiple Comparison Test.

A

	HCC827 GR6	EBC1 7A	MGH010	HN11 GR	H1975 R2	PC9 GR1	PC9 T790M PFR2	MDA-MB-453 LR1	MGH006 PFR1	MGH025
Primary RTK only	33.46	24.23	14.63	18.95	7.48	19.12	2.40	5.30	3.73	1.76
+ Gefitinib (1 μM)	30.42	4.32	10.54	13.55	9.30	17.99	2.49	5.05	2.08	0.64
+ Afatinib (0.25 μM)	29.44	3.20	12.54	13.57	7.90	12.87	1.26	3.72	2.04	0.49
+ OSI906 (1 μM)	23.63	24.55	9.86	4.79	8.26	10.38	0.07	5.03	3.14	1.11
+ MGCD265 (1 μM)	1.55	22.95	15.70	12.69	7.77	17.07	3.61	3.88	4.15	1.32
+ GDC0941 (0.25 μM)	24.57	17.07	8.70	8.67	8.23	13.34	0.28	1.43	3.59	0.30
+ AZD6244 (1 μM)	5.04	11.19	9.61	6.18	7.70	2.25	0.26	5.11	3.67	0.70
+ AZD0530 (1 μM)	22.87	3.24	2.73	4.34	7.75	15.39	1.98	5.69	1.00	0.22
+ Dasatinib (0.1 μM)	10.99	0.77	0.07	1.36	4.33	6.79	1.08	5.20	1.25	0.06
+ SNS314 (0.1 μM)	7.83	7.53	1.95	0.83	0.20	0.89	0.04	2.16	1.09	0.74
+ AZD1152 (0.25 μM)	5.71	6.60	2.02	0.94	0.13	0.98	0.04	2.08	1.30	0.57
+ ABT263 (1μM)	22.71	18.40	10.26	8.80	1.84	12.60	0.23	6.19	1.02	0.01

B

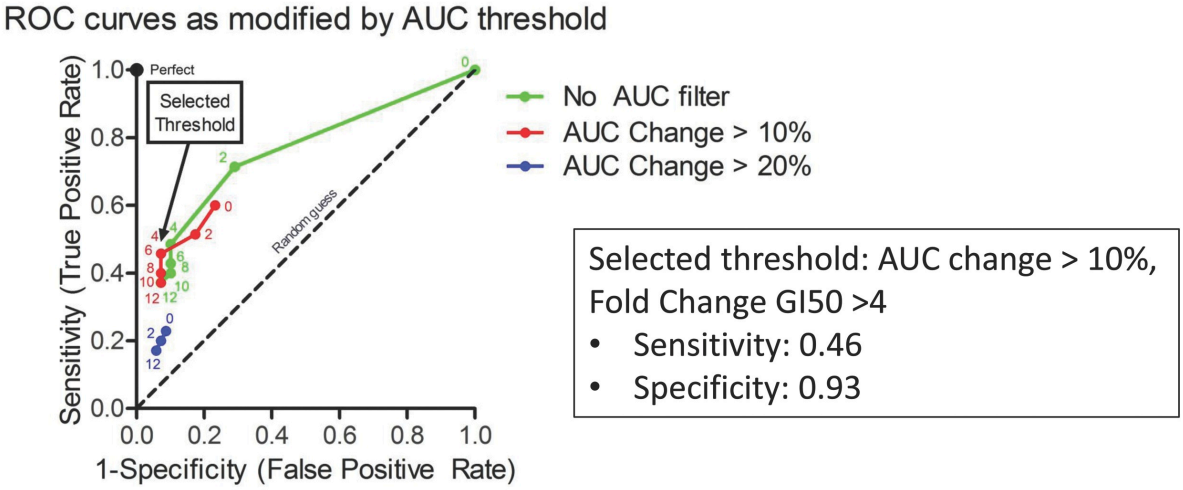

Fig. S16: Determination of thresholds to determine screen hits. A. Long-term viability assay was performed with 5 replicates per sample. Cell viability at day 6 was compared with viability at 0 (before initiation of treatment). Presented is the mean relative change in cell number that resulted in each cell line/drug combination. A combination was deemed effective if cells regressed or increased less than 1.6-fold from time=0. The experiment was performed once. **B.** Using LTV data as the gold standard, ROC curves were generated to determine the optimal threshold to define a screen "hit". Each line represents the ROC for various AUC based filters: No AUC filter (green), AUC change > 10% (red), AUC change > 20% (blue). Along the AUC curve the cutoff of fold-change in GI50 is presented.

	Sample Type	Successes	Failures	Success Rate (%)
EGFR	Biopsy	11	26	29.7
	Fluid	17	9	65.4
ALK	Biopsy	10	8	55.6
	Fluid	10	5	66.7
	Total	48	48	50.0

Table S1. Success rates for attempted model derivation from EGFR mutant and ALK-positive NSCLC samples from either biopsy (core biopsy or excisional biopsy) or from malignant extracellular fluid collection (ascites or pleural effusion).

.

Cell Line	Sex	Age	Oncogene	Targeted Rx	Duration of Rx (m)	Biopsy site	Oncogene sequence (Tumor)	Oncogene sequence (cell line)	Screen TKI
MGH006-1A	M	51	EML4-ALKv1	-		Pleural Effusion	EML4-ALKv1, wt	EML4-ALKv1, wt	Crizotinib (1 μM)
MGH010-1A	F	75	EML4-ALKv1	Crizotinib	8.4	AP window node	EML4-ALKv1, wt	EML4-ALKv1, wt	Crizotinib (1 μM)
MGH021-2B	M	22	SQSTM1-ALK	Crizotinib	27.4	Pleural Effusion	SQSTM1-ALK 1151Tins, G1269A	SQSTM1-ALK 1151Tins, G1269A	Crizotinib (1 μM)
MGH022-2A	F	73	EML4-ALKv2	Crizotinib	6.4	Ascites	EML4-ALKv2, wt	EML4-ALKv2, wt	Crizotinib (1 μM)
MGH025-1A	M	65	EML4-ALKv1	Crizotinib	11.5	Liver	EML4-ALKv1, wt	EML4-ALKv1, wt	Crizotinib (1 μM)
MGH034-2A	F	38	EML4-ALKv5	1. Crizotinib 2. Ceritinib	8.4 9.7	Liver	EML4-ALKv5, wt	EML4-ALKv5, wt	Ceritinib (300 nM)
MGH044-1B	M	56	EML4-ALKv2	Crizotinib	6.2	Liver	EML4-ALKv2 wt, amp	EML4-ALKv2 wt, amp	Crizotinib (1 μM)
MGH045-1A	M	66	EML4-ALKv1	Crizotinib	14.5	Pleural biopsy	EML4-ALKv1, L1196M	EML4-ALKv1, L1196M	Ceritinib (300 nM)
MGH049-1A	F	29	EML4-ALKv1	1. Crizotinib 2. Ceritinib	13.7 6.9	Pleural Effusion	EML4-ALKv1, wt	EML4-ALKv1, wt	Crizotinib (1 μM)
MGH051-1A	F	47	EML4-ALKv3	Crizotinib	2.8	Liver	EML4-ALKv3, wt	EML4-ALKv3, wt	Crizotinib (1 μM)
MGH003-1A	M	61	EGFR exon 19 del	Erlotinib	1.67	Pleural Fluid	exon 19 del, T790 wt	exon 19 del, T790 wt	Gefitinib (1μM)
MGH121-1A	F	43	EGFR exon 19 del	Erlotinib	6.8	Pleural Fluid	exon 19 del, T790M	exon 19 del, T790M	WZ4002 (1μM)
MGH126-1A	F	76	EGFR exon 19 del	Erlotinib	7.7	Pleural Fluid	insufficient material	exon 19 del, T790 wt	Gefitinib (1μM)
MGH131-4A	M	42	EGFR exon 19 del	1. Erlotinib 2. 2nd Generation TKI	6.4 3.0	Lung	exon 19 del, T790 wt	exon 19 del, T790 wt	Gefitinib (1μM)
MGH134-1A	M	70	EGFR exon 21, L858R	Erlotinib	8.4	Pleural Fluid	exon 21, L858R, T790M	exon 21, L858R, T790M	WZ4002 (1μM)
MGH141-1A	M	64	EGFR exon 19 del	Erlotinib	6.3	Pleural Fluid	exon 19 del, T790M	exon 19 del, T790M	WZ4002 (1μM)
MGH154-2B	M	67	EGFR exon 19 del	Erlotinib	17.1	Pleural Fluid	exon 19 del, T790 wt	exon 19 del, T790 wt	Gefitinib (1μM)
MGH156-1A	F	69	EGFR exon 19 del	1. Erlotinib 2. Cetuximab	14.4 7.0	Lung	exon 19 del, T790 wt	exon 19 del, T790 wt	Gefitinib (1μM)
MGH157-1A	M	64	EGFR exon 19 del	Erlotinib	12.3	Bone	exon 19 del, T790M	exon 19 del, T790M	WZ4002 (1μM)
MGH164-2C	M	52	EGFR exon 19 del	Erlotinib	9.9	Pleural Fluid	exon 19 del, T790M	exon 19 del, T790M	WZ4002 (1μM)
MGH170-1BB	F	76	EGFR exon 21, L858R	Erlotinib	8.8	Breast Mass	exon 21 L858R, T790 wt	exon 21 L858R, T790 wt	Gefitinib (1μM)

Table S2. Patient-derived resistant models: Patient and model characteristics.

Generic Name	Brand Name	Alt Drug Name	Primary Target (for screen)	Other targets	Stage
Vandetanib	Caprelsa	AZD6474/Zactima	RET	VEGFR/EGFR	Approved
Afatinib	Gilotrif	BIBW2992, Tomtovok, Tovok	ERBB (pan)		Approved
Tasocitinib	Xeljanz	Tofacitinib, CP-690550	JAK3		Approved
Vismodegib	Erivedge	GDC0449	SMO/HH		Approved
Gefitinib	Iressa		EGFR		Approved
Ruxolitinib	Jakafi	INCB018424	JAK1/2		Approved
Dasatinib	Sprycel	BMS-354825, Sprycel	SRC, ABL	EPHB, SFKs	Approved
Imatinib	Gleevec	STI-571, KIN001-014	ABL	ABL, KIT, PDGFR	Approved
Lapatinib	Tykerb		ErbB2		Approved
Crizotinib	Xalkori	PF2341066	ALK	MET	Approved
Vemurarinib	Zelboraf	PLX4720	BRAF	cRAF	Approved
Pyrimethamine	Daraprim		STAT3		Approved
Sorafenib	Nexavar		RAF	RAF, KIT, VEGFR, PDGFR	Approved
Sutent	Sunitinib		VEGFR		Approved
Temsirolimus	Torisel		mTOR		Approved
Bortezomib	Velcade		Proteasome		Approved
Vorinostat	Zolinza	SAHA	HDAC inhibitor Class I, IIa, IIb, IV		Approved
NVP-BGJ-398			FGFR family		Phase II
SNS 314			AURK (pan)		Phase I
AP26113			ALK	EGFR	PhaseI/II
MGCD-265			TIE2	MET, VEGFR, RON	Phase I/II
Navitoclax		ABT-263	BCL-2 family		Phase II
Veliparib		ABT888	PARP1/2		Phase II
BEZ235			PI3K	mTOR	Phase II
Alvocidib		Flavopiridol	CDK2, CDK7, CDK8, CDK9		Phase II
GDC0941			PI3K class 1		Phase II
BI-2536		KIN001-124, NPK33-1-98-1	PLK 1,2,3		Phase II
MK-2206			AKT		Phase II
NVP-BYL-719			p110a_PI3K		Phase II
Fostamatinib		R406	SYK		Phase II
RAF265		CHIR-265	RAF(A,B,C)	VEGFR2	Phase II
YM155			Survivin		Phase II
Tozasertib		VX-680, KIN001-006, MK0457	FLT3	Aurora	Phase II
AZD1152-HQPA			AURKB	FLT3, JAK2, RET	Phase II/III
Saracatinib		AZD0530, KIN001-045	SRC	ABL	Phase II/III
Olaparib		AZD2281, KU-0059436	PARP1/2		Phase III
Selumetinib		AZD6244, ARRY 142886	MEK 1/2		Phase III
Lestaurtinib		CEP-701	TRKA	FLT3, JAK2, RET	Phase III
Elesclomol		STA-4783	HSP70		Phase III
Midostaurin		PKC412	FLT3	KIT, PKC, VEGFR, PDGFR, MDR	Phase III
MLN8237			AURKA		Phase III
AICAR			AMPK (agonist)		Phase III
Linsitinib		OSI-906	IGF1R		Phase III
Palbociclib		PD-0332991	CDK4/6		Phase III
Dacomitinib		PF299804	ERB (pan)		Phase III
Zarnestra		Tipifarnib	Farnesyl Transferase		Phase III
Dovitinib		CHIR-258, TKI258	FGFR3		Phase III
Zibotentan		ZD4054	ETA-receptor		Phase III
Embelin			XIAP		PC
681640		Wee1 Inhibitor	WEE1, CHK1		PC
AEW541			IGFR		PC
AZ628			RAF(A,B,C)	BRAF>CRAF	PC
AZ960			JAK2		PC
BAY-1942		BAY 65-1942	IKK-beta		PC

Cyclopamine			SMO		PC
Geldanamycin			HSP90		PC
GSK 650394			SGK		PC
GW 5074			RAF (cRAF)		PC
IC87114			p110d_PI3K		PC
CGP60474		KIN001-019	CDK1,2,5,7,9		PC
WH-4-025		KIN001-113	SRC		PC
BMS-536924		KIN001-126	IGFR		PC
KIN001-135			IKK-epsilon		PC
GSK269962A		KIN001-155	Rho Kinase		PC
CT 99021		CHIR 99021, KIN001-157	GSK3		PC
KU55933			ATM		PC
LBW242			IAP		PC
LFM-A13/DDE-28			BTK	PLK	PC
MRK 003			g-Secretase		PC
PHA665752			MET		PC
QS11			ARFGAP		PC
R428			AXL		PC
RO-3306			CDK1		PC
SL 0101-1			RSK	AURKB, PIM3	PC
TGX221			p110b_PI3K		PC
TP-155		Triterpenoid	NFkB Signal		PC
XAV-939			Tankyrase 1 and 2		PC

Table S3. List of drugs used in the screen. The drug targets as well as the status of clinical development are listed. List of drugs used in the screen. The drug targets as well as the status of clinical development are listed.

Category	Primary Targets	Drugs
1	EGFR family	Gefitinib (EGFR), Lapatinib (HER2), Vandetanib (EGFR), BIBW2992 (EGFR/HER2), PF299804 (EGFR/HER2)
	ALK	Crizotinib (ALK, MET), AP26113 (ALK)
	MET	PHA665752 (MET), MGCD265 (MET)
	IGFR	BMS-536924 (IGFR), AEW541 (IGFR), OSI-906 (IGFR)
	RTK - Other	Dovitinib (FLT3), Midostaurin (FLT3), Lestaurtinib (NTRKA), Sunitinib (VEGFR), BGJ398(FGFR)
	Non-receptor TK	Imatinib (ABL), INCB018424 (JAK1/2), AZ960 (JAK2), LFM-A13 (BTK), Tasocitinib (JAK3), R406 (SYK), Dasatinib (SRC, ABL), AZD0530 (SRC, ABL), KIN001-113 (SRC)
2	Ser/Thr Kinase	SL0101-1 (RSK), GSK269962A (ROCK), CHIR99021 (GSK3), GSK650394 (SGK), AICAR (AMPK), KIN001-135 (IKKE), BAY-1942 (IKKB)
	PI3K pathway	TGX221 (p110b), IC87114 (p110d), BYL719 (p110a), GDC0941 (panPI3K), BEZ235 (panPI3K, mTOR), MK-2206 (AKT), Temsirolimus (mTOR)
	MAPK	PLX4720 (BRAF), AZ628 (RAF), GW 5074 (cRAF), RAF265 (panRAF), AZD6244 (MEK), Sorafenib (panRAF)
	Post-translational modification	XAV939 (Tankyrase), Tipifarnib (Farnesyl transferase)
3	Aurora Kinase	SNS314 (panAurora), MLN8054 (AuroraA), AZD1152 (AuroraB), VX680 (panAurora)
	Cell Cycle - Other	CGP60474 (CDK1,2,5,7,9), R0-3306 (CDK1), Flavopiridol (CDK2,7,8,9), PD-0332991 (CDK4,6), AZ83146 (TTK), BI2536 (PLK)
4	Transcription	Pyrimethamine (STAT3), TP-155 (NFKB), Vorinostat (HDAC)
5	Apoptosis	YM155 (survivin), ABT263 (BCL2), Embelin (XIAP), LBW242 (IAP)
6	Protein Folding and Stability	Velcade (Proteasome), Geldanamycin (HSP90), Elesclomol (HSP70)
7	Development, Differentiation	Cyclopamine (SMO), GDC0449 (SMO), ZD4054 (ETA), MRK003 (g-secretase), QS11 (ARFGAP)
8	DNA Damage Repair	Veliparib (PARP), Olaparib (PARP), 681649 (Wee1), KU55933 (ATM)

Table S4.

Screen drugs by target category. Drug set: The rationale for selection is listed as the potential mechanism for bypass of sensitivity to original TKI. Multiple levels of signaling as well as key cell fate decision modules were targeted. Categories: 1. Receptor / Upstream signal activation; 2. Intracellular signaling pathway; 3. Cell Cycle Control Bypass; 4. Transcriptional Bypass; 5. Apoptosis regulation; 6. Protein Stress and Chaperoning; 7. Differentiation Escape; and 8. DNA Damage Stressors.

Parent Line	Resistant Line	Cancer Type	Resistance	Oncogene	Known genetics of parental line	Acquired alteration	Acquired bypass	Screen TKI
HCC827	HCC827 GR6	NSCLC (adneo)	Gefitinib	EGFR ex19del		MET amplication	MET	Gefitinib (1 μM)
A431	A431 GR	Cervical (SCC)	Gefitinib	EGFR (amplification)			IGF1R	Gefitinib (1 μM)
HN11	HN11 GR	HNSCC	Gefitinib	EGFR (amplification)			IGF1R	Gefitinib (1 μM)
PC9	PC9 GR1	NSCLC (adeno)	Gefitinib	EGFR ex19del	TP53 R248Q			Gefitinib (1 μM)
PC9	PC9 GR2	NSCLC (adeno)	Gefitinib	EGFR ex19del	TP53 R248Q	EGFR T790M		Gefitinib (1 μM)
PC9	PC9 GR3	NSCLC (adeno)	Gefitinib	EGFR ex19del	TP53 R248Q	EGFR T790M		Gefitinib (1 μM)
PC14	PC14 GR1	NSCLC (adeno)	Gefitinib	EGFR ex19del				Gefitinib (1 μM)
PC14	PC14 GR2	NSCLC (adeno)	Gefitinib	EGFR ex19del				Gefitinib (1 μM)
PC14	PC14 GR3	NSCLC (adeno)	Gefitinib	EGFR ex19del				Gefitinib (1 μM)
H4006	H4006 GR	NSCLC	Gefitinib	EGFR ex19del				Gefitinib (1 μM)
PC9 GR2	PC9 T790M PFR2	NSCLC (adeno)	Dacomitinib	EGFR ex19del T790M	TP53 R248Q, EGFR T790M			Dacomitinib (1 μM)
H3255	H3255 GR	NSCLC (adeno)	Gefitinib	EGFR L858R				Gefitinib (1 μM)
H1975	H1975 PFR2	NSCLC (adeno)	Dacomitinib	EGFR L858R T790M				Dacomitinib (1 μM)
H3122	H3122 CR3	NSCLC (adeno)	Crizotinib	EML4-ALK			EGFR	Crizotinib (1 μM)
H3122	H3122 x4.2	NSCLC (adeno)	Crizotinib	EML4-ALK				Crizotinib (1 μM)
H2228	H2228 PFR1	NSCLC (adeno)	Crizotinib	EML4-ALK				Crizotinib (1 μM)
H2228	H2228 PFR1 LS	NSCLC (adeno)	Crizotinib	EML4-ALK				Crizotinib (1 μM)
MGH006	MGH006 PFR1	NSCLC (adeno)	Crizotinib	EML4-ALK				Crizotinib (1 μM)
MGH006	MGH006 PFR2	NSCLC (adeno)	Crizotinib	EML4-ALK				Crizotinib (1 μM)
MDA-MB453	MDA-MB453 LR1	Breast carcinoma	Lapatinib	HER2	PIK3CA H1047R, FGFR Y367C, CDH1 W638*			Lapatinib (1 μM)
MDA-MB453	MDA-MB453 LR2	Breast carcinoma	Lapatinib	HER2	PIK3CA H1047R, FGFR Y367C, CDH1 W638*			Lapatinib (1 μM)
MDA-MB453	MDA-MB453 LR3	Breast carcinoma	Lapatinib	HER2	PIK3CA H1047R, FGFR Y367C, CDH1 W638*			Lapatinib (1 μM)
SKBR3	SKBR3 LR1	Breast carcinoma	Lapatinib	HER2				Lapatinib (1 μM)
SKBR3	SKBR3 LR2	Breast carcinoma	Lapatinib	HER2				Lapatinib (1 μM)
SKBR3	SKBR3 LR3	Breast carcinoma	Lapatinib	HER2				Lapatinib (1 μM)
AU565	AU565 LR1	Breast carcinoma	Lapatinib	HER2				Lapatinib (1 μM)
AU565	AU565 LR2	Breast carcinoma	Lapatinib	HER2				Lapatinib (1 μM)
AU565	AU565 LR3	Breast carcinoma	Lapatinib	HER2				Lapatinib (1 μM)
H1819	H1819 LR1	NSCLC (adeno)	Lapatinib	HER2	SMARCA1 L1085fs*32			Lapatinib (1 μM)
UACC893	UACC893 LR2	Breast carcinoma	Lapatinib	HER2	PIK3CA H1047L, CDH1 H233Q			Lapatinib (1 μM)
UACC893	UACC893 LR3	Breast carcinoma	Lapatinib	HER2	PIK3CA H1047L, CDH1 H233Q			Lapatinib (1 μM)
SNU638	SNU638 A1	Gastric adeno	PHA665752	MET	CTNNB1 T41A	Y1230H		PHA665752 (1 μM)
SNU638	SNU638 C1	Gastric adeno	PHA665752	MET	CTNNB1 T41A		EGFR	PHA665752 (1 μM)
SNU638	SNU638 C2	Gastric adeno	PHA665752	MET	CTNNB1 T41A		EGFR	PHA665752 (1 μM)
EBC1	EBC1 1A	NSCLC (SCC)	PHA665752	MET				PHA665752 (1 μM)
EBC1	EBC1 4B	NSCLC (SCC)	PHA665752	MET				PHA665752 (1 μM)
EBC1	EBC1 7A	NSCLC (SCC)	PHA665752	MET				PHA665752 (1 μM)
MKN45	MKN45 SR1	Gastric adeno	PHA665752	MET	EGFR A1048V			PHA665752 (1 μM)
MKN45	MKN45 SR2	Gastric adeno	PHA665752	MET	EGFR A1048V			PHA665752 (1 μM)
MKN45	MKN45 SR3	Gastric adeno	PHA665752	MET	EGFR A1048V			PHA665752 (1 μM)

Table S5. Characteristics of cell line models of acquired resistance derived *in vitro* by chronic treatment with TKI.

Cell line	Control	2° EGFR mutation	Gene	AA change	cDNA change	Allelic fraction	SNP frequency (1000 genomes)
MGH121-1A	Blood	T790M	TP53	F109S	326T>C	0.99	0
MGH126-1A	HapMap		TP53	M237I	711G>T	1	0
			TRIO	S2767L	8300C>T	0.288	0.000458
MGH131-4A	Blood		TP53	R273L	818G>T	0.992	0
MGH134-1A	Blood	T790M	RNASEL	A102V	305C>T	0.031	0
			TP53	R342*	1024C>T	1	0
MGH141-1A	Blood	T790M	TP53	N247I	740A>T	1	0
MGH156-1A	HapMap		AR	Q58L	173A>T	0.147	0
			EIF2AK4	E734D	2202G>C	0.279	0
			FGFR3	Y649C	1946A>G	0.387	0
MGH157-1A	Blood	T790M, L747S, R748K	ICK	R336*	1006C>T	0.424	0
			TP53	H179R	536A>G	0.997	0

Table S6. Mutations in patient-derived *EGFR* mutant cell lines identified by NGS.

Cell line	Control	2° ALK mutation	Gene	cDNA change	AA change	Allelic fraction	SNP frequency (1000 genomes)
MGH010-1A	HapMap		HSP90AB1	2156G>A	R719H	0.053	0
MGH021-2B	HapMap	G1269A	ADAMTSL3	1295T>C	V432A	0.485	0.000458
			CDK4	409G>A	V137I	0.436	0
			JAK2	1711G>A	G571S	0.208	
			JAK3	2164G>A	V722I	0.293	0.003663004
MGH022-2A	HapMap		APC	3949G>C	E1317Q	0.532	0.003663004
			CSF1R	95T>G	V32G	0.559	0.000916
			HSP90AB1	2156G>A	R719H	0.05	0
			MAP3K11	2189G>A	R730H	0.683	0.005494505
			TP53	560G>T	G187V	0.994	0
MGH025-1A	Blood		SMAD4	1255G>A	G419R	0.993	0
MGH034-2A	HapMap		ASXL1	3306G>T	E1102D	0.526	0.009157509
			CUBN	8741C>T	A2914V	0.526	0.005952381
			JAK3	2164G>A	V722I	0.532	0.003663004
			MAP2K1	171G>T	K57N	0.446	0
			TP53	832C>T	P278S	0.98	0
MGH044-1B	HapMap		MELK	947C>T	T316I	0.606	0.009615385
			NPR1	1621G>A	G541S	0.436	0.000916
			TP53	638G>A	R213Q	0.975	0
MGH045-1A	HapMap	L1196M	ADCK4	187C>T	R63W	0.345	0.003205128
			ATM	8083G>A	G2695S	0.426	0
MGH049-1A	HapMap		ITGB5	1847C>T	T616M	0.495	0.002747253
			NF1	4708G>T	E1570*	1	0
MGH051-1A	Blood		SDHD	359T>C	L120S	0.045	0
H3122 CR3	H3122		CDH1	2284G>T	E762*	0.135	0
			IGF2R	2284G>T	E762*	0.063	0
MGH006-1A PF1	MGH006		None				
MGH006-1A PF2	MGH006		None				

Table S7. Mutations in patient-derived ALK-positive cell lines identified by NGS.

Cell line	Drug	Condition or Outcome	C1	C2	C3	C4	C5	C6	C7	C8	C9	Q1	Average	Min
MGH010	AZD0530	Excess over Bliss	-6%	-3%	-4%	-15%	-33%	-36%	-49%	-38%	-21%	-36%	-24%	-49%
MGH025	AZD0530	Excess over Bliss	-5%	-3%	-8%	-12%	-9%	-18%	-18%	-19%	-18%	-18%	-13%	-19%
MGH034	AZD6244	Excess over Bliss	-15%	-20%	-39%	-37%	-57%	-56%	-62%	-60%	-50%	-57%	-45%	-62%
MGH044	AZD0530	Excess over Bliss	-1%	-9%	-7%	-3%	-16%	-18%	-18%	-22%	-8%	-18%	-12%	-22%
MGH045	AZD0530	Excess over Bliss	5%	3%	-1%	-7%	-17%	-24%	-20%	-15%	-5%	-17%	-10%	-24%
MGH049	AZD0530	Excess over Bliss	-7%	-10%	-7%	-22%	-27%	-42%	-36%	-24%	-5%	-27%	-21%	-42%
MGH156-1A	BGJ398	Excess over Bliss	-3%	-3%	-3%	-7%	-5%	-17%	-22%	-24%	-19%	-19%	-12%	-24%
MGH170-1BB	Crizotinib	Excess over Bliss	-24%	-28%	-35%	-27%	-26%	-32%	-27%	-18%	-8%	-28%	-25%	-35%
PC9 GR1	AZD6244	Excess over Bliss	-4%	-12%	-19%	-25%	-30%	-31%	-26%	-16%	-15%	-26%	-20%	-31%
PC9 T790M PF2	ABT-263	Excess over Bliss	1%	0%	-3%	-12%	-16%	-13%	-7%	-5%	0%	-12%	-7%	-16%
MGH010	AZD0530	Expected Bliss Combination	75%	66%	76%	80%	86%	77%	64%	48%	25%			
MGH025	AZD0530	Expected Bliss Combination	85%	74%	70%	61%	47%	43%	30%	21%	19%			
MGH034	AZD6244	Expected Bliss Combination	111%	108%	106%	94%	94%	87%	84%	79%	57%			
MGH044	AZD0530	Expected Bliss Combination	70%	72%	67%	64%	66%	60%	53%	47%	28%			
MGH045	AZD0530	Expected Bliss Combination	39%	44%	46%	45%	44%	40%	31%	24%	12%			
MGH049	AZD0530	Expected Bliss Combination	67%	64%	66%	65%	54%	52%	43%	30%	8%			
MGH156-1A	BGJ398	Expected Bliss Combination	35%	36%	35%	36%	34%	36%	36%	34%	26%			
MGH170-1BB	Crizotinib	Expected Bliss Combination	60%	58%	59%	50%	50%	55%	48%	26%	9%			
PC9 GR1	AZD6244	Expected Bliss Combination	68%	67%	67%	61%	57%	52%	40%	26%	20%			
PC9 T790M PF2	ABT-263	Expected Bliss Combination	25%	24%	24%	23%	20%	13%	8%	5%	0%			
MGH010	AZD0530	Observed Combination	69%	63%	71%	65%	53%	41%	15%	10%	4%			
MGH025	AZD0530	Observed Combination	80%	71%	62%	49%	38%	25%	12%	2%	1%			
MGH034	AZD6244	Observed Combination	96%	88%	68%	56%	37%	30%	22%	19%	8%			
MGH044	AZD0530	Observed Combination	68%	63%	60%	61%	50%	42%	35%	25%	20%			
MGH045	AZD0530	Observed Combination	44%	47%	45%	38%	27%	16%	11%	9%	7%			
MGH049	AZD0530	Observed Combination	60%	54%	59%	43%	27%	10%	7%	6%	3%			
MGH156-1A	BGJ398	Observed Combination	33%	34%	32%	29%	29%	19%	14%	9%	6%			
MGH170-1BB	Crizotinib	Observed Combination	36%	30%	25%	23%	24%	23%	21%	8%	1%			
PC9 GR1	AZD6244	Observed Combination	64%	55%	48%	37%	28%	21%	14%	10%	5%			
PC9 T790M PF2	ABT-263	Observed Combination	27%	24%	21%	12%	4%	1%	0%	0%	0%			
MGH010	AZD0530	Single Agent	131%	116%	132%	140%	151%	134%	113%	85%	44%			
MGH025	AZD0530	Single Agent	94%	81%	77%	67%	52%	48%	33%	23%	21%			
MGH034	AZD6244	Single Agent	101%	98%	97%	85%	86%	79%	76%	72%	52%			
MGH044	AZD0530	Single Agent	94%	97%	90%	86%	89%	81%	72%	63%	38%			
MGH045	AZD0530	Single Agent	101%	116%	119%	119%	115%	104%	82%	63%	31%			
MGH049	AZD0530	Single Agent	109%	103%	107%	105%	87%	84%	69%	48%	12%			
MGH156-1A	BGJ398	Single Agent	97%	101%	97%	99%	95%	101%	100%	93%	72%			
MGH170-1BB	Crizotinib	Single Agent	95%	92%	94%	79%	78%	87%	76%	41%	15%			
PC9 GR1	AZD6244	Single Agent	87%	85%	85%	78%	73%	66%	51%	33%	25%			
PC9 T790M PF2	ABT-263	Single Agent	97%	93%	92%	89%	76%	51%	30%	19%	1%			

Table S8. Evaluation of synergism using the Bliss independence model. For each cell line and treatment the viability ratio (or the difference from expected viability) compared to untreated DMSO control is indicated. Expected Bliss values correspond to the calculation based on the Bliss independence model (see methods). Drug: single agent used in combination with the TKI matching each model (EGFR or ALK inhbibitor). C1-C9: Viability measured (Observed), expected (Expected Bliss) or difference from expected viability (Excess over Bliss) at each concentration tested. Q1: First quartile value, corresponding to the third maximum excess over Bliss value. Average: average of excess over Bliss values across all concentrations. Min: Minimum excess over Bliss value across all tested concentration corresponding to maximum synergism.

Additional Database S1-S8:

Supplementary Database 1: Next generation sequencing data for ALK cell lines

Supplementary Database 2: Next generation sequencing data for EGFR cell lines

Supplementary Database 3: GI50s of all screened cell line models as single agent and in combination

Supplementary Database 4: Fold Change GI50

Supplementary Database 5: Percent decrease in AUC

Supplementary Database 6: Upregulated and downregulated probe sets in GEA analysis

Supplementary Database 7: Downregulated gene list, DAVID analysis
Supplementary Database 8: Upregulated genelist, DAVID analysis

References

1. A. Inoue *et al.*, Prospective phase II study of gefitinib for chemotherapy-naive patients with advanced non-small-cell lung cancer with epidermal growth factor receptor gene mutations. *J Clin Oncol* 24, 3340 (Jul 20, 2006).

2. E. L. Kwak *et al.*, Anaplastic lymphoma kinase inhibition in non-small-cell lung cancer. *N Engl J Med* 363, 1693 (Oct 28, 2010).

3. R. Rosell *et al.*, Erlotinib versus standard chemotherapy as first-line treatment for European patients with advanced EGFR mutation-positive non-small-cell lung cancer (EURTAC): a multicentre, open-label, randomised phase 3 trial. *Lancet Oncol* 13, 239 (Mar, 2012).

4. L. V. Sequist *et al.*, First-line gefitinib in patients with advanced non-small-cell lung cancer harboring somatic EGFR mutations. *J Clin Oncol* 26, 2442 (May 20, 2008).

5. A. T. Shaw *et al.*, Effect of crizotinib on overall survival in patients with advanced non-small-cell lung cancer harbouring ALK gene rearrangement: a retrospective analysis. *Lancet Oncol* 12, 1004 (Oct, 2011).

6. C. R. Chong, P. A. Janne, The quest to overcome resistance to EGFR-targeted therapies in cancer. *Nat Med* 19, 1389 (Nov, 2013).

7. R. Katayama *et al.*, Mechanisms of acquired crizotinib resistance in ALK-rearranged lung Cancers. *Sci Transl Med* 4, 120ra17 (Feb 8, 2012).

8. N. Yamaguchi *et al.*, Dual ALK and EGFR inhibition targets a mechanism of acquired resistance to the tyrosine kinase inhibitor crizotinib in ALK rearranged lung cancer. *Lung Cancer* 83, 37 (Jan, 2014).

9. J. Tanizaki *et al.*, Activation of HER family signaling as a mechanism of acquired resistance to ALK inhibitors in EML4-ALK-positive non-small cell lung cancer. *Clin Cancer Res* 18, 6219 (Nov 15, 2012).

10. M. J. Niederst, J. A. Engelman, Bypass mechanisms of resistance to receptor tyrosine kinase inhibition in lung cancer. *Sci Signal* 6, re6 (Sep 24, 2013).

11. X. Liu *et al.*, ROCK inhibitor and feeder cells induce the conditional reprogramming of epithelial cells. *Am J Pathol* 180, 599 (Feb, 2012).

12. J. A. Engelman *et al.*, Effective use of PI3K and MEK inhibitors to treat mutant Kras G12D and PIK3CA H1047R murine lung cancers. *Nat Med* 14, 1351 (Dec, 2008).

13. J. A. Engelman *et al.*, MET amplification leads to gefitinib resistance in lung cancer by activating ERBB3 signaling. *Science* 316, 1039 (May 18, 2007).

14. A. C. Faber *et al.*, Differential induction of apoptosis in HER2 and EGFR addicted cancers following PI3K inhibition. *Proc Natl Acad Sci U S A* 106, 19503 (Nov 17, 2009).

15. M. L. Sos *et al.*, Identifying genotype-dependent efficacy of single and combined PI3K- and MAPK-pathway inhibition in cancer. *Proc Natl Acad Sci U S A* 106, 18351 (Oct 27, 2009).

16. M. Guix *et al.*, Acquired resistance to EGFR tyrosine kinase inhibitors in cancer cells is mediated by loss of IGF-binding proteins. *J Clin Invest* 118, 2609 (Jul, 2008).

17. J. Qi *et al.*, Multiple Mutations and Bypass Mechanisms Can Contribute to Development of Acquired Resistance to MET Inhibitors. *Cancer Res*, (Jan 25, 2011).

18. L. V. Sequist *et al.*, Genotypic and histological evolution of lung cancers acquiring resistance to EGFR inhibitors. *Sci Transl Med* 3, 75ra26 (Mar 23, 2011).

19. T. H. Marsilje *et al.*, Synthesis, Structure-Activity Relationships, and in Vivo Efficacy of the Novel Potent and Selective Anaplastic Lymphoma Kinase (ALK) Inhibitor 5-Chloro-N2-(2-isopropoxy-5-methyl-4-(piperidin-4-yl)phenyl)-N4-(2-(isopropylsulf onyl)phenyl)pyrimidine-2,4-diamine (LDK378) Currently in Phase 1 and Phase 2 Clinical Trials. *J Med Chem*, (Jun 26, 2013).

20. A. T. Shaw *et al.*, Ceritinib in ALK-rearranged non-small-cell lung cancer. *N Engl J Med* 370, 1189 (Mar 27, 2014).

21. J. L. Marks *et al.*, Novel MEK1 mutation identified by mutational analysis of epidermal growth factor receptor signaling pathway genes in lung adenocarcinoma. *Cancer Res* 68, 5524 (Jul 15, 2008).

22. D. K. Walters *et al.*, Activating alleles of JAK3 in acute megakaryoblastic leukemia. *Cancer Cell* 10, 65 (Jul, 2006).

23. M. W. Karaman *et al.*, A quantitative analysis of kinase inhibitor selectivity. *Nat Biotechnol* 26, 127 (Jan, 2008).

24. U. McDermott, R. V. Pusapati, J. G. Christensen, N. S. Gray, J. Settleman, Acquired resistance of non-small cell lung cancer cells to MET kinase inhibition is mediated by a switch to epidermal growth factor receptor dependency. *Cancer Res* 70, 1625 (Feb 15, 2010).

25. L. F. Hennequin *et al.*, N-(5-chloro-1,3-benzodioxol-4-yl)-7-[2-(4-methylpiperazin-1-yl)ethoxy]-5- (tetrahydro-2H-pyran-4-yloxy)quinazolin-4-amine, a novel, highly selective, orally available, dual-specific c-Src/Abl kinase inhibitor. *J Med Chem* 49, 6465 (Nov 2, 2006).

26. S. Bagrodia, I. Chackalaparampil, T. E. Kmiecik, D. Shalloway, Altered tyrosine 527 phosphorylation and mitotic activation of p60c-src. *Nature* 349, 172 (Jan 10, 1991).

27. L. Friboulet *et al.*, The ALK inhibitor ceritinib overcomes crizotinib resistance in non-small cell lung cancer. *Cancer Discov*, (Mar 27, 2014).

28. H. Ebi *et al.*, Receptor tyrosine kinases exert dominant control over PI3K signaling in human KRAS mutant colorectal cancers. *J Clin Invest* 121, 4311 (Nov, 2011).

29. R. Katayama *et al.*, Therapeutic strategies to overcome crizotinib resistance in non-small cell lung cancers harboring the fusion oncogene EML4-ALK. *Proc Natl Acad Sci U S A* 108, 7535 (May 3, 2011).

30. L. Gautier, L. Cope, B. M. Bolstad, R. A. Irizarry, affy--analysis of Affymetrix GeneChip data at the probe level. *Bioinformatics* 20, 307 (Feb 12, 2004).

31. G. K. Smyth, Linear models and empirical bayes methods for assessing differential expression in microarray experiments. *Statistical applications in genetics and molecular biology* 3, Article3 (2004).

32. W. Huang da, B. T. Sherman, R. A. Lempicki, Systematic and integrative analysis of large gene lists using DAVID bioinformatics resources. *Nature protocols* 4, 44 (2009).

33. M. Zhao, J. Sun, Z. Zhao, TSGene: a web resource for tumor suppressor genes. *Nucleic Acids Research*, 41, D970 (2013).

34. U. McDermott *et al.*, Genomic alterations of anaplastic lymphoma kinase may sensitize tumors to anaplastic lymphoma kinase inhibitors. *Cancer Res* 68, 3389 (May 1, 2008).